PDR

BNL-NUREG-31754
Limited Distribution

INFORMAL REPORT

NRC Research and/or Technical Assistance Rept

UNIFORM, PITTING AND CREVICE CORROSION, AND HYDROGEN EMBRITTLEMENT TEST REQUIREMENTS FOR TICODE-12 HIGH LEVEL WASTE CONTAINERS

DRAFT REPORT

H. JAIN

MANUSCRIPT COMPLETED AUGUST 1982

NUCLEAR WASTE MANAGEMENT DIVISION
DEPARTMENT OF NUCLEAR ENERGY BROOKHAVEN NATIONAL LABORATORY
UPTON, NEW YORK 11973

Prepared for the U.S. Nuclear Regulatory Commission
Office of Nuclear Materials Safety and Safeguards
Contract No. DE-AC02-76CH00016

BNL-NUREG-31754
INFORMAL REPORT
Limited Distribution

UNIFORM, PITTING AND CREVICE CORROSION, AND HYDROGEN EMBRITTLEMENT TEST REQUIREMENTS FOR TiCode-12 HIGH LEVEL WASTE CONTAINERS

DRAFT REPORT

H. Jain

Manuscript Completed August 1982

Prepared by
The Nuclear Waste Management Division
D. G. Schweitzer, Head
Department of Nuclear Energy
Brookhaven National Laboratory
Associated Universities, Inc.
Upton, NY 11973

Prepared for the U.S. Nuclear Regulatory Commission
Office of Nuclear Materials Safety and Safeguards
Contract No. DE-AC02-76CH00016
FIN No. A-3167

NOTICE

ABSTRACT

This report is a review of the relevant test methods to show compliance with the approximately 1000-year containment criterion of a TiCode-12 container undergoing uniform, pitting and crevice corrosion, and hydrogen embrittlement in a basalt or a salt repository. The general testing considerations common to all four types of failure modes are discussed first, followed by the specific details pertinent to each mode. The salt repository conditions are generally expected to be more corrosive than those of the basalt repository. A major problem with the test methods is to find suitable accelerating conditions and be able to extrapolate the data to repository situations. The corrosion life of the container may be determined using direct or electrochemical methods, the latter being particularly helpful in understanding the mechanisms.

Uniform corrosion is not expected to be the major corrosion problem, but its understanding as a function of various parameters will help in evaluating other types of corrosion. Pitting on TiCode-12 has not been observed to date. Testing for much longer durations under more corrosive conditions will be needed to confirm this observation. Crevice corrosion in brine has been only recently observed and needs to be tested further under better defined conditions. Hydrogen from fabrication processes or radiolysis of groundwater can be seriously detrimental to the TiCode-12 container. Fracture mechanics tests starting with the determination of the threshold stress intensity factor K_{Th} are needed; other tests will be useful to supplement this information under elastic-plastic conditions.

CONTENTS

FIGURES

ACKNOWLEDGMENT

The author is grateful to J. Shao, P. Soo, T. M. Ahn, B. S. Lee, and B. Siskind for their helpful suggestions and comments. He also wishes to express his appreciation to Ms. Sharon M. Moore and Ms. Grace Searles for their efforts in the preparation of this report.

1. INTRODUCTION

TiCode-12, (0.8% Ni, 0.3% Mo, balance Ti) is a leading candidate material for use as a high level waste container alloy. It shows superior corrosion resistance compared to other alloys of titanium, stainless steels, Inconel, etc.[1] However, the available data to characterize possible modes of failure of TiCode-12 are not sufficient, and additional information is required[2] to show that this alloy will meet the NRC 1000-year waste containment criterion. The purpose of this report is to review the existing uniform, pitting, and crevice corrosion, and hydrogen embrittlement tests in relation to salt and basalt repository conditions, and then further identify tests which should be performed in order to demonstrate that TiCode-12 will meet the 1000-year containment requirement. Considerations common to all the four kinds of tests are presented in the next two sections. This is followed by discussions specific to each mode of failure.

1.1 Relevant Environmental Variables

Two kinds of repositories are presently under consideration for this report: (a) a salt repository where the container may come in contact with brine and (b) a basalt repository where it may come in contact with basaltic groundwater. Besides this basic difference, there are other variables, namely, temperature, pH, Eh, composition, and flow rate of the corroding groundwater; radiation, and new products generated due to irradiation, which must be considered in a laboratory test to simulate the field conditions.

Siskind and Hsieh[3] have recently reviewed near-field conditions for basalt and salt repositories. Their report lists available information on the ranges of different parameters which are likely to influence the life of TiCode-12. Temperature, pressure, and changes due to irradiation are the parameters common to both kinds of repositories. Groundwater chemistry and hydraulic properties are of concern with the basalt repository, whereas brine inclusion migration is specific to a salt repository. To ensure compliance of TiCode-12 to the containment criterion, respective corrosion and hydrogen embrittlement tests should be performed over the anticipated ranges of each of the above mentioned parameters. This will provide suitable data for extrapolation, to prototypic repository design conditions.

Some of the parameters may influence the corrosion life of TiCode-12 indirectly. For example, the temperature dependence of the uniform corrosion rate may be larger in a lower pH solution. Such interactions need to be considered to determine overall corrosion rates.

The presently available information on either basalt or salt repository conditions is not complete,[3] which means that the respective testing conditions are also ill defined. The lack of information is most importantly due to uncertainties in the final design of the high level waste package itself. For example, relevant repository conditions will be vastly different depending on whether a radiation shield is used in the container system.

Shaw and Soo[4] have reviewed available uniform and pitting corrosion data for TiCode-12 under different conditions. Though TiCode-12 has shown superior resistance to uniform and pitting corrosion, it is concluded that not all the possible repository conditions have been given enough attention. Major areas where further information is needed are:

- Effect of gamma radiation directly on the corrosion process or indirectly through changes in the corroding atmosphere due to radiolysis, etc.
- Correlation between microstructural variables of the alloy and corrosion rates.
- Stability of the oxide film which is primarily responsible for the corrosion resistance of TiCode-12
- Reliability of the predictions of the lifetime of TiCode-12, based on data which are collected only during the very early stage of corrosion.

Similar conclusions are drawn by Lee and Ahn for crevice corrosion and hydrogen embrittlement, respectively. The details of these data requirements are included in FIN A-3164 reports[2] under preparation.

1.2 General Experimental Considerations

To perform corrosion testing under the high temperature and high pressure conditions expected for the repositories, special laboratory apparatus is needed. Berry[5] has discussed the basic types of testing arrangements, including autoclaves with a window or irradiation accessories. The experimental setup used at Rockwell International[6] and Pacific Northwest Laboratory (PNL)[7] are shown in Figures 1 and 2, respectively, for corrosion tests in simulated groundwater. For basalt repository conditions, as used at these organizations, one needs a high pressure autoclave system where a flow of solution is maintained. In the PNL setup, the groundwater was purged with N_2 or argon and passed through a column of basalt to create oxygen fugacity comparable to what is found in repository water. However, it was noted by Anderson[6] that crushed basalt did not produce equilibrium values of oxygen concentration. In this respect, Hart[8] has discussed the use of a galvanic cell to evaluate and then control the concentration of dissolved oxygen in the brine.

The uniform corrosion results reported from experiments at Rockwell International and PNL are preliminary; only weight changes for several alloys are reported without defining what these represent in terms of actual metal thickness loss. PNL plans to perform further tests under gamma radiation conditions (see Figure 3). The system at Rockwell International (Figure 1) appears to have a good access capability for solution analysis; the addition of an irradiation facility would be highly desirable.

Brine inclusions in salt repository have much smaller movement compared to water in a basalt repository. Therefore, having an autoclave with flowing brine is not necessary. BNL,[9] PNL,[7] and Sandia National Laboratories

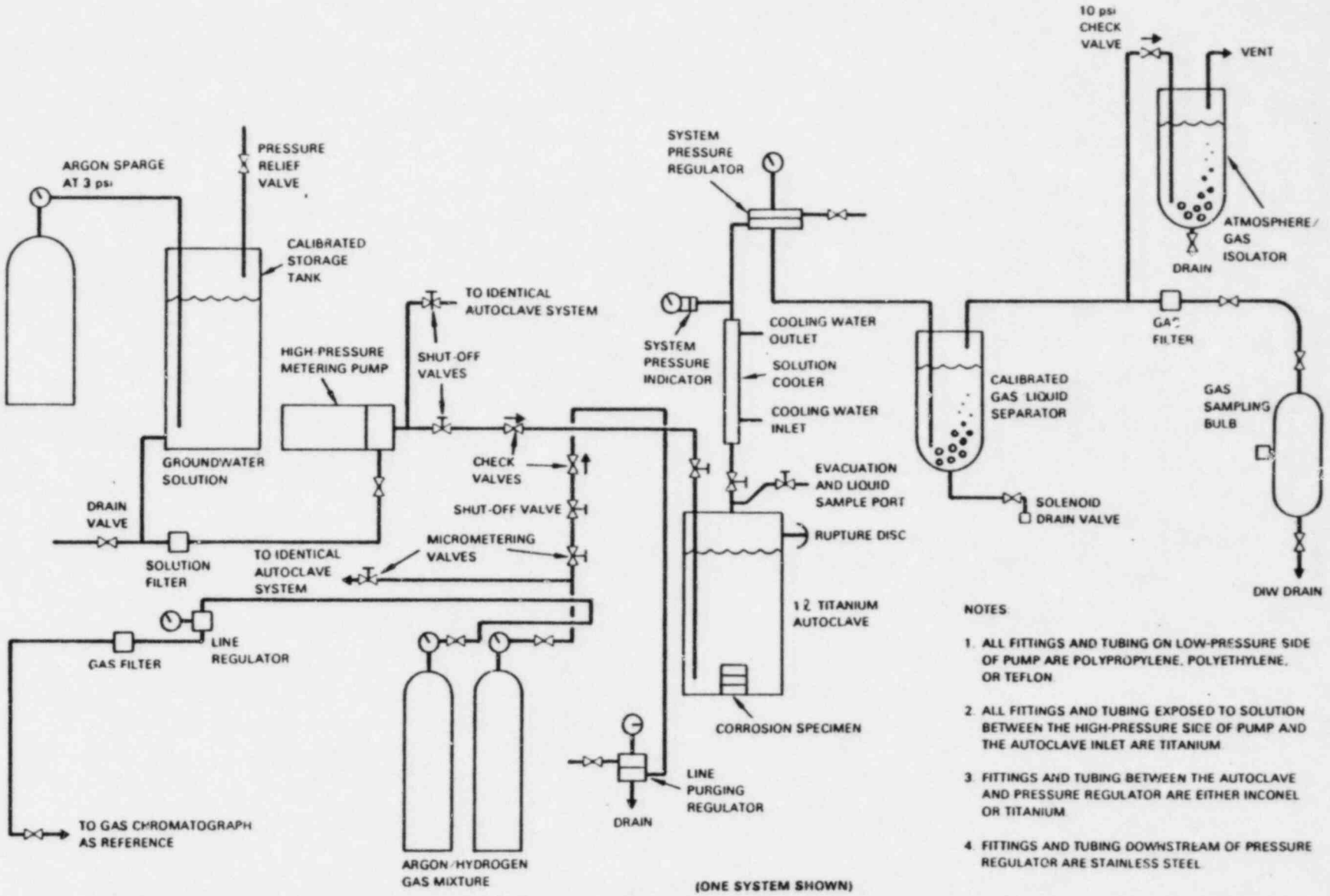

Figure 1. Rockwell corrosion testing system for container/overpack materials screening tests.[6]

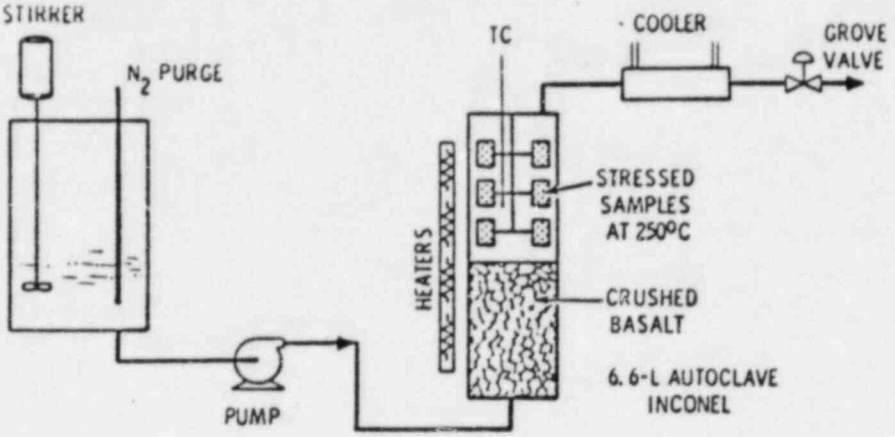

Figure 2. PNL autoclave system.[7]

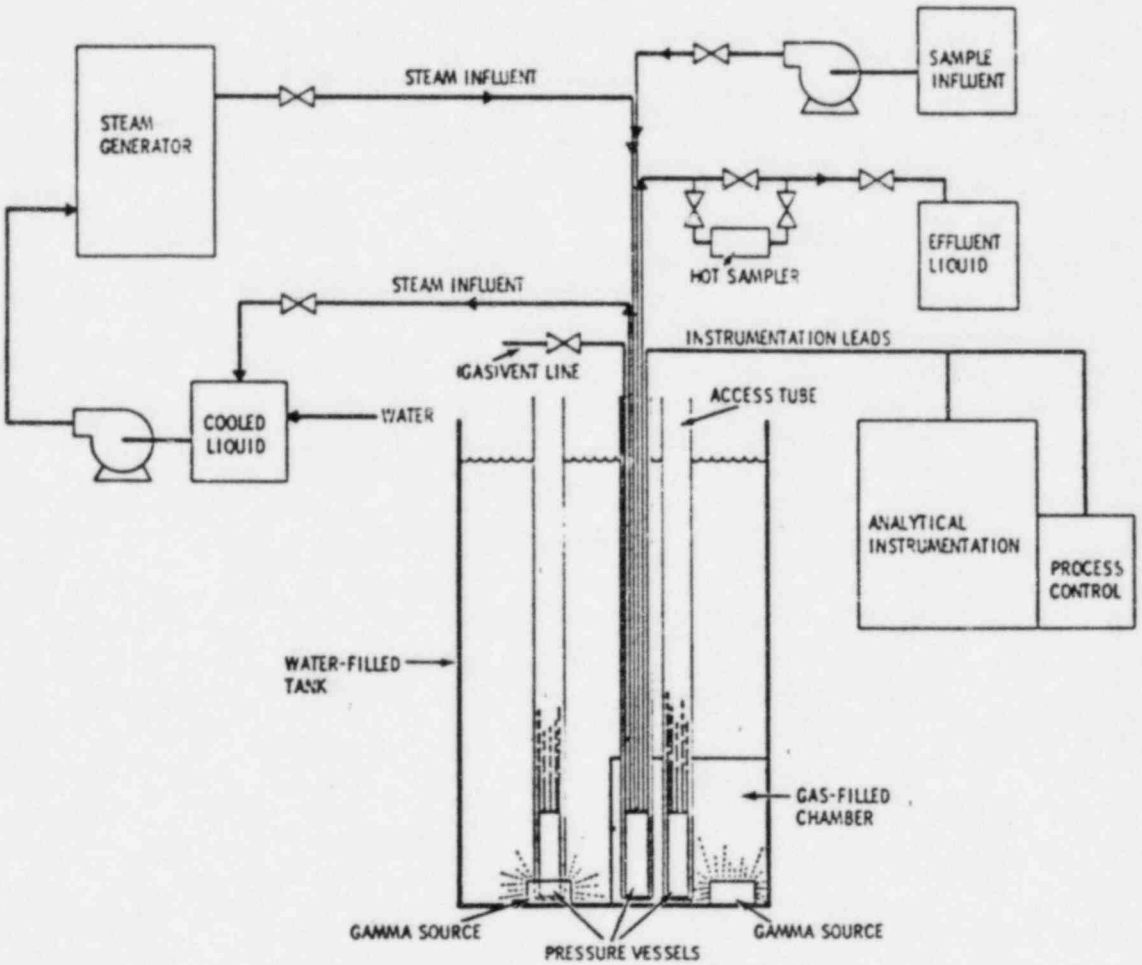

Figure 3. PNL radiation test facility.[7]

(SNL)[10] have used closed systems, producing static corrosion data. Corrosion of TiCode-12 in geothermal brines is also being evaluated both in static[11] and flowing autoclaves. The brines used in these tests are different from brines considered typical of salt repositories. Nevertheless, some of the experimental details are common and can be considered for corrosion in repository brines.

The material of the system in which corrosion tests are to be carried out, should ideally have negligible corrosion rates compared to that of the test specimens. When system corrosion is not negligible, corrosion products from the system can interfere with the sample corrosion process and produce incorrect results. For example, oxides of nickel and molybdenum originating from a Hastelloy autoclave were found to be deposited on TiCode-12 specimens in oxygenated brine.[10] Such deposition will not only give an incorrect change in weight of the sample, but may also affect the corrosion/passivation mechanism. PTFE teflon is a commonly used liner material which does not corrode at room temperature. However, at elevated temperatures (>200°C), teflon must be used with caution. Titanium or TiCode-12 liners for autoclaves may be an alternative. In summary, one should take precautions in selecting the testing equipment material so that it does not interfere with the corrosion process of the samples.

WIPP Brine A is a commonly used test solution which is considered to be representative of a salt repository. It is more corrosive[12] than WIPP Brine B or seawater presumably due to its lower pH at high temperature. Compositions of these brines and seawater are listed in Table 1. The compositions listed in this table are indicative of equilibrium concentrations of various chemical species at room temperature. At elevated temperatures, the equilibrium concentration will be much higher due to higher solubility of various salts. For example, the fraction of total dissolved solids in Brine A at 25°C is 25.46 weight percent (using a density of 1.202 g/cc)[13] which increases to 34.0 weight percent at 200°C. Further, it is concluded that bitterns near the waste containers will most probably contain 35 to 55 weight percent total dissolved solids and values as high as 75 weight percent are possible.[13] Clearly, the presently performed corrosion experiments at high temperatures in Brine A grossly underestimate the concentration of corrosive species which the container may encounter in a salt repository. Therefore, it is suggested that some testing be conducted as a function of temperature in brines which are in equilibrium at that temperature.

Temperature, radiation, and pressure are the major parameters which should be explicitly considered in evaluating corrosion of TiCode-12. Of these, the effect of radiation is least studied. For example, radiation will change the corrosion rate mainly by altering the chemistry of brines by radiolysis. The production of NaOH and hydrogen due to irradiation of salt has been postulated.[15] In this regard, one may consider two cases: (1) effect of radiation on brine and (2) effect of radiation on solid salt which eventually reacts with brine. The radiolysis products may or may not be the same for the two cases. It will be useful to check this point before continuing with elaborate experimentation with radiation.

Table 1

Representative Corrosion Solution Compositions
(Major Ions)

Ion	Seawater (ppm)	Brine A[a] (ppm)	Brine B[b] (ppm)
Na^+	10,651	42,000	115,000
K^+	380	30,000	15
Mg^{+2}	1,272	35,000	10
Ca^{+2}	400	600	900
Sr^{+2}	13	5	15
Cl^-	18,980	190,000	175,000
SO_4^{-2}	884	3,500	3,500
I^-	0.05	10	10
HCO_3^-	146	700	10
Br^-	65	400	400
BO_3^{-3}	--	1,200	10
pH[c]	8.1	6.5	6.5
Eh[d]	--	mildly oxidizing	mildly oxidizing
Total Dissolved Solids	35 g/L	306 g/L	297 g/L

[a]Brine A is a high Mg, K, and Na chloride brine and is representative of water which might intrude into the proposed (WIPP) site by percolation through an overlying zone containing potash. It is also considered tentatively representative of minute brine inclusions found in bedded salt formations.

[b]Brine B is a nearly saturated, predominately NaCl brine representative of dissolved, bedded salt at the 800 m horizon of the proposed WIPP site.

[c]These pH values are taken at room temperature; they decrease with increasing temperature (e.g., seawater solution quenched from 270°C measured 3.3 at room temperature).

[d]From Reference 14.

When groundwater or brine reaches the container, its composition might also be modified due to the presence of backfill material such as bentonite. An earlier BNL report[4] suggested that such composition variations will be small and can be checked in an in situ waste package test. However, a simple experiment demonstrating that brine composition does not change significantly after coming in contact with the backfill material at appropriate temperature and pressure will be a desirable first step.

TiCode-12 has superior corrosion resistance compared to unalloyed titanium, presumably due to a change in anodic potential at the alloy surface caused by the alloying elements. Details of this mechanism are not known. Chemical analysis of specimens of TiCode-12 at BNL has shown[9] considerable variation in the concentrations of iron and nickel. This compositional variation is likely to affect the corrosion rates of TiCode-12. To compare the results of different investigators, the source of their material should be reported, and preferably the same material used until the influence of alloying elements on corrosion is understood.

2. TESTS FOR UNIFORM CORROSION

2.1 Introduction

In general, titanium and its alloys are very reactive; their surfaces readily transform into one of the oxides of titanium. The superior corrosion resistance of TiCode-12 is primarily due to the inertness and stability of this oxide film. When the oxide film is not stable, e.g., in air free dilute HCl or H_2SO_4 (where the corrosion potential is in the electrochemically active region) titanium corrodes rapidly. Determination of corrosion resistance of TiCode-12, therefore, concerns the properties of the oxide film during corrosion. Characterization of the oxide film under various corrosion conditions, though a very difficult task, is of vital importance.

Uniform corrosion tests should involve determination of the growth and/or dissolution rate of the oxide film as well as its stability. One may approach this problem either by focusing on the oxide film, or the remainder of the alloy not yet corroded. For the purpose of predicting the lifetime of the alloy, both approaches should be equally acceptable. Experimentally, the problems with each approach may be significantly different and one may obtain different results if the experimental conditions are not well understood.

In August of 1980, the Materials Characterization Center (MCC) held a workshop to prepare guidelines for corrosion testing of engineered barrier metals. The suggestions made by the MCC in its summary report[16] are not specific to TiCode-12, but most of these are applicable to this alloy. The MCC Workshop considered various available testing procedures and recommended that the following hierarchy may be adopted to determine uniform corrosion rates: (1) gravimetric tests, (2) polarization resistance tests, (3) surface analysis for film thickness, (4) metallurgical examination, (5) surface analysis for characterization, (6) interferometry and ellipsometry techniques, and (7) solution analysis. Each of these test procedures are relevant to TiCode-12 as discussed below.

2.2 Gravimetric Measurements

The gravimetric or weight change method of determining uniform corrosion is based on estimating the loss of metal or alloy by measuring its weight before and after corrosion. It is recommended that the surface finish, thermal history, etc. of the laboratory specimen be representative of the container to be used in the repository. To evaluate the effects of any microstructural or other changes during welding, additional testing on welded samples is necessary and may be carried out as suggested in the ASTM Standard Practice G58-78.[17]

In most cases, uniform corrosion produces oxide or some other form of loosely attached scale on the metal surface. In such cases, the loss in sample weight after removing the corrosion product is obtained to calculate the corrosion rate. The standard procedure for such a measurement is described in ASTM Designation G1.[18] In the case of TiCode-12 however, a strongly adhering oxide layer is formed. Removal of this oxide layer (which may be quite thin) can easily remove some of the metal as well, thus introducing a large error in weight loss. Discrepancies in the results of different authors[6,19] may be partly due to this reason. A preferred method for TiCode-12 would be to measure the gain in weight of the sample as the oxide layer is formed. However, note that the weight-gain method assumes: (1) all of the oxide adheres to the surface and (2) it does not dissolve in the corrosive solution.

Although uniform corrosion is often expressed as the change in weight for a given set of experimental conditions and test duration, for the purpose of estimating the life of a TiCode-12 container, it is more appropriate to describe corrosion in terms of loss of container thickness per year (μm/year). The conversion from weight-change to thickness-loss requires the knowledge of: (1) the area of the sample exposed to corrosive solution and (2) the nature of the corrosion film. The area of a sample is easy to determine, but the oxide film on TiCode-12 has hardly been characterized. In the simplest case, the weight gain is assumed entirely due to the addition of oxygen and thus the corresponding weight of titanium reacted with oxygen can be easily calculated if the type of oxide is known. From the weight of corroded titanium, finding the loss of thickness per year is straightforward.

In a complex system such as TiCode-12 in a brine containing 15 or more reactive ions, it is probably an incorrect assumption that corrosion produces only a TiO_2 film. For example, Braithwaite and others[10] have found oxides of nickel and molybdenum in the corrosion layer and Ahn and Soo[20] have found significant amounts of Mg and Si on the surface layer of TiO_2 formed from corrosion in WIPP Brine A. The latter authors also found that thickness of the film was twice the value predicted from weight measurements.

These observations suggest that for uniform corrosion of TiCode-12 in relevant solution, the weight gain cannot be easily converted to corrosion rate. To achieve such a conversion correctly, one should first correlate weight gain with loss of thickness of the alloy determined from an independent experiment.

As mentioned above, porosity of the film or adsorption of elements from solution, introduce error in the determination of alloy thickness lost due to corrosion. A more important consequence of adsorption of elements from solution is their effect on the stability of the oxide film. Such adsorption may mean that uniform corrosion does not produce an absolutely uniform oxide film and may lead to localized corrosion in time. This question will be considered further in the sections on non-uniform corrosion, but it may be noted that characterization of the oxide film produced by uniform corrosion is important even for other kinds of corrosion.

2.3 Electrochemical Measurements

2.3.1 Polarization Resistance Tests

The linear polarization technique is based on the relationship:[21]

$$I_{corr} = B/R_p$$

where I_{corr} is the corrosion current which is directly proportional to the uniform corrosion rate, R_p is the experimentally determined polarization resistance and B is a constant related to Tafel slopes of the cathodic and anodic processes.

The sample in the appropriate corroding solution is polarized by applying a voltage of a few mV from the corrosion potential and then measuring the resulting current. Assuming that Ohm's law is applicable, the ratio of the two gives R_p. There are commercial instruments available which measure R_p and convert the results directly to the uniform corrosion rate in mils per year. The measurement can be done remotely and the corrosion process monitored without removing the sample from the autoclave or corrosion system. Thus, this method appears to be a simple, easy to use technique.

Due to departure from Ohm's law and uncertainty in the value of B, the results from the linear polarization method are considered to be only reliable to within a factor of two.[21] Danielson[22] has found that when oxygen is introduced into the solution, one may underestimate actual corrosion rates by as much as a factor of five because the corrosion rate is now controlled by mass transport at the cathode. Unfortunately, the results of polarization resistance do not give any indication that the corrosion mechanism and hence the value of B, has changed considerably. This method has not been used on TiCode-12 either for salt or basalt repository conditions. Due to different chemistries and conditions in the two repositories, one would need to determine the value of constant B separately.

The polarization technique described above uses a dc signal. Detailed information about the corrosion mechanisms particularly in high resistivity groundwater can be obtained by measuring ac impedance over a wide range of frequencies. In several cases, the faradaic process is frequency dependent and one determines from "complex impedance analysis" the charge transfer resistance which then correlates well with the corrosion rate.[23,24]

2.3.2 Other Electrochemical Measurements

In these measurements, one determines the voltage-current (voltammogram) response of the corrosion system under the relevant conditions of pH, temperature, etc. The results can be used to predict the corrosion behavior of an alloy by comparing with the voltage that would be expected in an actual situation. For example, titanium samples having an oxide layer prepared by thermal oxidation and anodization show different corrosion resistances. This observation is directly connected with polarization characteristics.[25] The corrosion resistance of an oxide film under different conditions can be estimated from the magnitude of the corrosion current after passivation.

Common experimental instrumentation for potentiostatic or potentiodynamic measurements is relatively simple and commercially available. Standard procedures for these measurements are described by ASTM.[26] Substantial modification from the ASTM procedure is required to test TiCode-12 in a repository simulated environment. General problems of measurements above 100°C are discussed by Jones and Masterson.[27] Some measurements of TiCode-12 at high temperature and pressure using an autoclave are under way at BNL[9] and SNL.[10] These results are very preliminary, and further experiments will be required before drawing any conclusions regarding the mechanisms of corrosion.

MacDonald, Syrett, and others[28,29] have performed electrochemical measurements on TiCode-12 in geothermal brines at temperatures up to 250°C. Sweeping the voltage from the noble to the active region several times produces cyclic voltammograms such as that shown for TiCode-12 in Figure 4. From the complexity of Figure 4, it is clear that interpretation of such electrochemical measurements for alloys in complex corrosive solutions is not straightforward. However, cyclic voltammograms do indicate the changes which might be overlooked in a single sweeping of voltage. It is suggested here that to represent steady state behavior, the voltage sweeping rates be as slow as possible.

The corrosion potential for TiCode-12 was found[28] to become more active when the temperature of the brine was increased, but started to become nobler with time. It is believed that at higher temperatures, dissolved oxygen is consumed more readily and subsequent retardation in corrosion may be related to the formation of a surface film which inhibits the anodic reaction. Thus, the amount of dissolved oxygen is an important parameter and is reflected in the time dependence of voltammograms. It would be desirable to regulate the dissolved oxygen and then understand its effect on corrosion in a controlled manner. There are no experiments in basalt groundwater reported to date on voltammograms for TiCode-12. Due to fewer reactants than in brine, the data will probably be simpler and more useful. However, in this case, one would like to know explicitly the effect of dissolved oxygen on electrochemical parameters. Finally, in situations where enough supporting thermodynamic data about various reacting species in the corrosion solution are available (unfortunately to date not for TiCode-12), one can construct useful Pourbaix diagrams from voltammogram data (see Reference 28 and references therein).

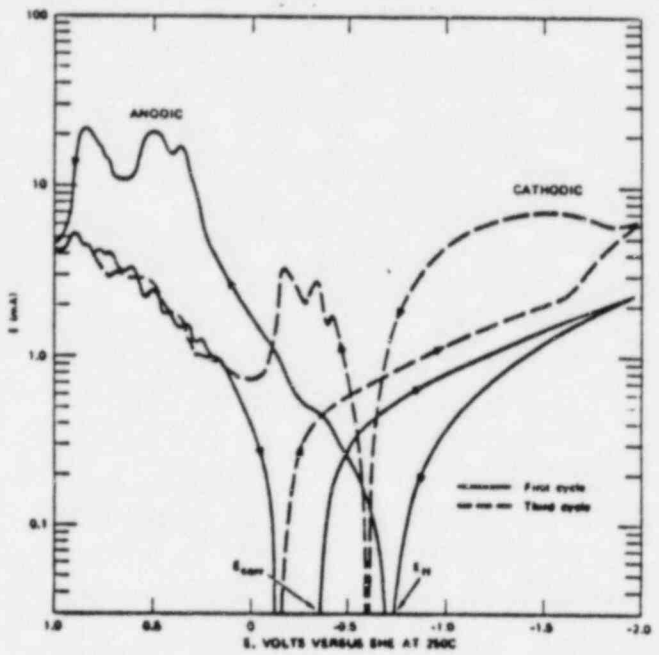

Figure 4. Cyclic voltammogram for TiCode-12 in high salinity brine at 250°C after 146 hours exposure.[28]

2.4 Film Thickness Measurements

Uniform corrosion of TiCode-12 involves the growth of an oxide film on its surface and to a limited extent dissolution of this oxide film. Hence, the change in the thickness of a sample due to corrosion is the direct measurement for this type of corrosion. The MCC Workshop has suggested[16] the following thickness measurement tests (in order of preference) for this purpose.

2.4.1 Surface Analyses

In this method, thickness of the oxide film is determined by sputtering the film off the sample. Since it is possible to perform this experiment in conjunction with Auger or electron spectroscopy for chemical analysis facilities, one can also study the composition and structure of the film. Sputtering is a complex phenomenon and its rate may depend both on chemical compositions and physical condition of the film. However, once the rate of sputtering is standardized for the given situation, the method can be easily used for similar specimens; corrosion specimens from basalt and salt solutions would probably need to be standardized separately. This method may be

particularly attractive for TiCode-12 corrosion where film thickness will usually be very small.

2.4.2 Metallographic Examinations

It is always desirable to examine a metallographically sectioned and polished corrosion sample under an optical microscope. This will confirm the uniformity of the corrosion film as well as show any development of nonuniform corrosion. One can use this method to determine corrosion films thicker than 1 μ. However, since the film thickness on TiCode-12 is usually very small, use of an optical microscope may not be the ideal technique for thickness determination.

2.4.3 Interference and Ellipsometry Methods

These optical methods are appropriate for very thin oxide films and possibly appropriate for TiCode-12 corrosion study. In interferometric methods, the thickness of the oxide film is measured in terms of interference-fringe shift due to the optical path difference with respect to uncorroded surfaces. Sometimes, however, the fringes are not significantly shifted and are difficult to relate to absolute thickness. This method has not been commonly used in the past and only should be considered for TiCode-12 corrosion under special circumstances.

The above mentioned oxide thickness determination methods examine the film after the completion of corrosion. The ellipsometric method, however, can be used for in situ measurements during the growth of the film. In this fashion, one can observe the kinetics of film growth at very early stages. There are no measurements currently available on TiCode-12, but a titanium-aluminum alloy has been studied using ellipsometry under external stress and voltage.[30] To investigate the uniform corrosion of TiCode-12, one would first need to determine the optical properties of the oxide film in relation to film thickness. Due to the possible deposition of some impurities from the corrosion solution, it is suggested that the films from basalt water and brine be calibrated separately if such techniques are employed.

2.5 Solution Analyses

In this method, uniform corrosion of an alloy is estimated from chemical analysis of the corrosion solution containing dissolved metal. Shortcomings of this technique were pointed out by the MCC.[16] For TiCode-12 corrosion in brine or basalt water, the corrosion solution is very complex and the dissolution rate of the alloy, if any, is very small. Therefore, this testing method is not expected to provide reasonably accurate uniform corrosion rates. However, chemical analysis of the solution may be useful to determine changes in solution such as those due to precipitation of compounds on specimens and autoclave walls.

2.6 Conclusions

Salient features, possible problems, and important precautions for the measurement of uniform corrosion of TiCode-12 using the general methods outlined by the MCC are discussed above. With this information, modifications of above methods in conjunction with new techniques can be readily adopted. For example, at BNL the thickness of oxide films on TiCode-12 after exposure to WIPP Brine A was determined by examining the transverse sections of the sample under the scanning electron microscope.[20] At the same time, energy dispersive spectroscopy techniques were used to identify any impurities in the corrosion scale. Since such instruments are versatile and very common, their usage may be preferred over the older techniques such as interferometry.

Most of the thickness measurement methods described above concentrate on the observation of the corrosion layer on TiCode-12. However, the basic parameter of interest is the loss in thickness of TiCode-12, which should be obtained as a function of time, temperature, radiation, pH, Eh, etc. One can measure this parameter most simply by examining the cross section of the corrosion sample. This is similar to the approach recently adopted at BNL except that the emphasis should be on the metal loss rather than the oxide growth. One may determine the alloy loss by measuring the position of its metallic surface from a pre-marked inert "reference", before and after corrosion. The "reference" can be a small part of the surface which was not exposed to corrosion, or a fine line on a side surface of the sample. Of course, it should be assured that the corrosion process is not altered due to the presence of the "reference".

3. TESTS FOR PITTING CORROSION

3.1 Introduction

Pitting is a form of corrosion where the metal corrodes locally, at discrete locations on the surface. It occurs where the passivating film breaks up locally, due to some flaw in the film, the metal below it, or even statistical fluctuation in corrosion solution. Thus, pitting is a highly statistical phenomenon, and testing results will depend on the area examined or number of the samples used. Extreme value statistical analysis[31] has been shown to reasonably predict the time of perforation of long metal tubes, from laboratory data on small samples.[32,33] The same analysis may be applied here, but first enough data on maximum pit depths should be collected to show that it obeys this analysis.

Since TiCode-12's corrosion resistance is due to the passivating TiO_2 film, this alloy may be susceptible to pitting. In general, pitting is aided by the chloride ions. Therefore, a salt repository environment will be much more conducive to pitting than basalt water. Currently available data have not shown any signs of pitting corrosion of TiCode-12 in either environment, though several variables (e.g., irradiation, Eh and water flow rate in basalt water, etc.) have not been evaluated.[4] It is a well known fact that pitting may occur after an induction or incubation period which is not known

for TiCode-12. The induction period may depend on the solution characteristics. Once started, a pit grows rapidly in an autocatalytic fashion. Long term tests on TiCode-12 should be carried out to determine the likelihood of pitting. It may be noted that due to the more corrosive environment inside a crevice, pitting could be more severe in this region.

The MCC summary report[16] has listed the methods for nonuniform corrosion testing by dividing them into conventional and nonconventional techniques in flowing or static solutions. The distinction between static and flowing solutions is important because pitting may depend on the flow rate, e.g., there is a decrease in the pitting of a stainless steel as the flow rate of seawater increases.[34] Apparently, the flowing solution changes the local conditions and the pit growth is arrested. However, uniform corrosion may be higher as the solution flow rate is increased. The MCC report has further identified following hierarchy of screening tests for pitting:

1. Mechanical breakdown of the passive layer
2. Sustained electrochemical tests
3. Immersion tests under chemical potentiostatic control
4. Systems tests.

The above hierarchy is reasonable if the ease and time for testing are considered and should be appropriate for screening purposes. The tests in the first two categories are accelerated by externally applied mechanical or electrochemical perturbation. Besides being much faster, these tests are also appropriate for understanding the mechanisms of pitting. Important features and problems of all the test methods in the above categories are discussed next for pitting of TiCode-12 in basalt and salt repositories. General experimental considerations for pitting tests are almost the same as for uniform corrosion discussed earlier and are, therefore, not repeated here; only relevant differences will be pointed out.

3.2 Test Methods

3.2.1 Mechanical Breakdown of the Passive Layer

Since pitting is a result of local breakdown of the passivating layer, one can study the pitting behavior of TiCode-12 by artificially rupturing the titanium oxide film in a limited area (to maintain large cathode/anode area ratio) and observe the changes in surface properties. Ahn and others[9] have made use of this test on titanium and TiCode-12 in 1 M HCl at 80°C. A scratch was made on the surface of these alloys using a diamond tipped scriber. From the open circuit potential transient measurement on a fully abraded surface the active/passive state of the sample could be determined as a function of time. These measurements were relatively fast and particularly useful in comparing the performance of titanium and TiCode-12, and may be used to compare TiCode-12 corrosion resistance in various solutions. So far only preliminary testing has been done using the "scratch" method.

The method described above will provide some information about the mechanisms of pitting on TiCode-12. In this regard, it will be useful to produce a single pit and simultaneously observe it under an optical microscope. Bech and Chan[34] have studied growth of small pits on stainless steel in this fashion. The flow rate of corrosion solution was varied in their experimental setup, which could be of use for tests relevant to a basalt repository. Alternatively, one may simply rotate the specimen at varying speeds if solution chemistry does not change during the test.

3.2.2 Sustained Electrochemical Tests

One purpose of an electrochemical test is to determine potential vs current characteristics of a corrosion cell for given conditions. An example is shown[35] in Figure 5 for titanium in chloride solution. Pitting occurs when a specific potential is reached. It is often necessary to identify the potential at which pitting starts and the one at which a pit repassivates; the two are different because it takes a more corrosive environment to initiate a pit than to sustain an established pit. When enough information is collected from polarization curves, regimes of passivation and pitting may be obtained as a function of test conditions.

There are several variations for electrochemical testing,[36] but these may be divided into two broad categories, namely, controlled current and controlled potential. In the former, constant current is passed through a corrosion cell and the potential of the specimen is measured. The polarization curve is then obtained by changing the applied current, either in steps (galvanostatic) or by continuous sweeping (galvanodynamic). In many cases the sweeping rate will affect the current-potential response of the cell; the time dependence of potential (or current) may be useful information to describe the kinetics of pit growth.[37] In the case of controlled potential, one applies a predetermined potential on the specimen and measures the resulting current. Due to the different time responses for the two types of tests, each has its own advantages and disadvantages.[38] For metals which show an active/passive transition such as TiCode-12, the constant potential (potentiostatic or potentiodynamic) technique is most commonly used. However, it is useful to compare the results with galvanodynamic data, as was demonstrated in the determination of pitting and repassivation potentials of Incoloy in water containing chloride and phosphate ions.[39] Braithwaite and others[10] have carried out some potentiodynamic measurements of passive layer breakdown potential of TiCode-12 in seawater, Brine A, and Brine B. Increasing temperature showed the strongest adverse effect, then lack of oxygen, followed by increasing salt content.

To obtain an estimate of the effect of surface preparation on the susceptibility of TiCode-12 to pitting, the "anodic breakdown residual potential test" (ABRPT) method by Murphy[40] may be used. It is a galvanodynamic method in which the potential of the sample is measured as the applied current is gradually (within one hour) increased to 1000 μA. The minimum value of potential after anodic breakdown is taken as a measure of pitting susceptibility.

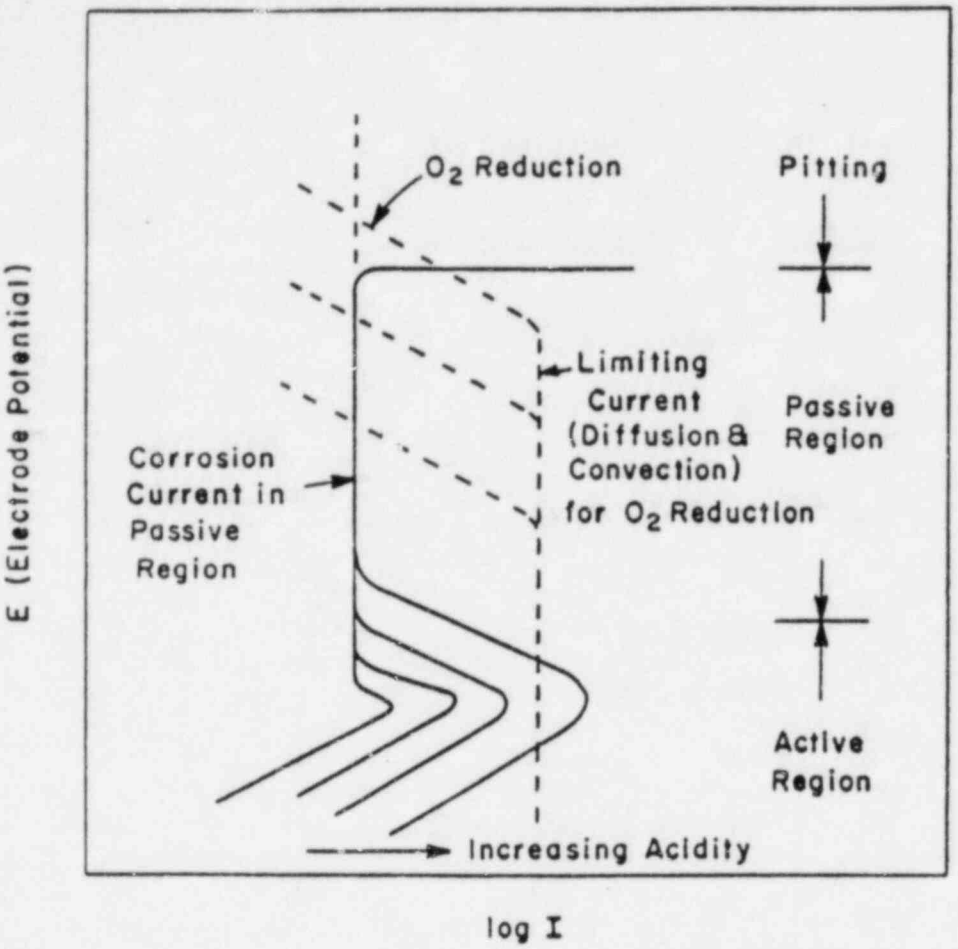

Figure 5. Schematic diagram of polarization curves for commercially pure titanium in chloride solution.[35]

It cannot be overemphasized that electrochemical data are best suited for making comparisons of the pitting tendency of TiCode-12 under different conditions. The results may depend on the surface condition, rate of measurement, solution conditions, etc. Very often this makes it very difficult to compare results from different laboratories. Sometimes the mechanisms of pitting may be different in the actual situation and accelerated laboratory tests. Therefore, a correlation between actual pitting and electrochemical observations must be established for the latter to be directly useful. Nevertheless, several recently developed electrochemical and other techniques possess excellent capabilities to study the mechanisms of pitting. They are briefly described below:

- During pitting corrosion current flows between the anodic area inside the pit and the cathodic part of the sample. Figure 6 illustrates how the potential may vary across a pit on an inhomogeneous surface. The potential distribution on a pitting sample can be measured by scanning the sample surface with a microtip electrode.[41,42] Alternatively, the microelectrode is kept fixed and a cylindrical sample is rotated

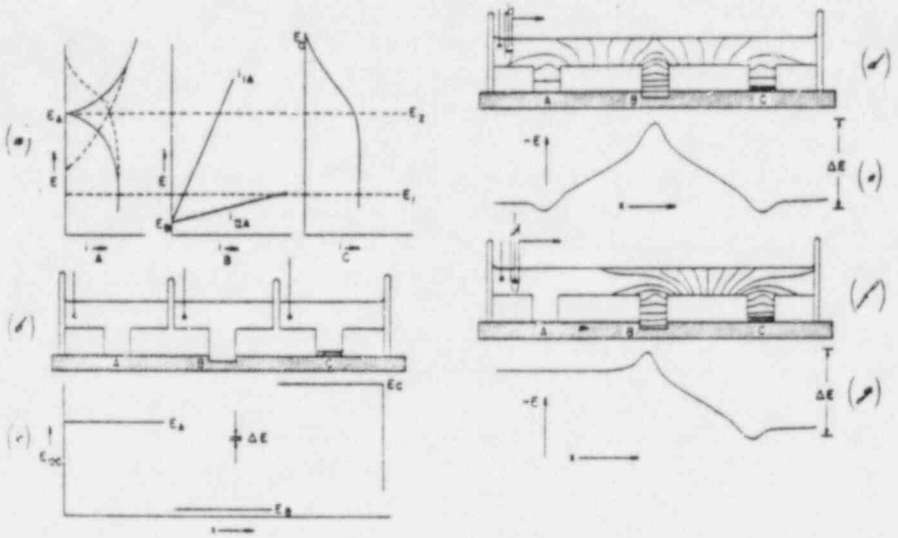

(a) Polarization diagrams for each exposed area
A - passive surface supporting anodic and cathodic reactions
B - local "pitting" anode with either high (I) or low (II) polarization
C - metal-coated area supporting only a cathodic reaction.
(b) Areas exposed to separate solutions.
(c) Open-circuit potentials in solutions between "iron" and the reference electrodes.
(d) Equipotential lines in solution when area B has low polarization (II).
(e) Potential variations on scanning across the sample for case (d).
(f) Equipotential lines in solution when area B has high polarization (I).
(g) Potential variations on scanning across the sample for case (f).

Figure 6. Schematic variations of the potential in a solution above a partially coated "iron" surface.[41]

to scan its circumference.[43] The testing system can be designed to map the potential across the whole surface directly, but is not available commercially. If it is possible to correlate the observed potential peak at the center of a pit to the corrosion current, the technique may be used to quantitatively determine pitting characteristics.

- Alternating current impedance measurements[44] are often used in corrosion studies to understand elementary processes such as dissolution, passivation, inhibition, mass transfer, etc. These measurements are particularly useful for high resistivity solutions, but so far a direct correlation between ac results and pitting has not been established.

Pitting on TiCode-12 results from local failure of the titanium oxide film. Therefore, the structure, stability, composition, etc. of this film should be characterized to understand the pitting phenomenon. It is not possible to achieve this goal with the exclusive use of the electrochemical techniques described above, and one should consider using modern surface analysis techniques to complement the electrochemical information. Optical and electron microscopy for film morphology, X-ray emission and electron spectroscopy for composition and film thickness, reflection high energy electron diffraction (RHEED) for the structure of the film, and Auger spectroscopy in conjunction with sputtering for layer by layer structure can virtually provide all the supporting information one might need for film characterization. By comparing the results of surface analysis techniques with the observed electrochemical conditions of various stages of pitting, one can predict the pitting with greater confidence or even suggest appropriate methods to improve pitting resistance (see Reference 45). Initially, such experiments will have to be limited to simpler corrosion conditions than expected for TiCode-12 in a repository, or the result may become too complex to be interpreted.

3.2.3 Immersion Tests Under Chemical Potentiostatic Control

These tests may be performed in the laboratory by exposing the specimens to the test solutions and allowing them to pit unaided by external electrochemical potentials. The pitting corrosion may then be evaluated following ASTM Standard Recommended Practice.[46] The first step would be to obtain morphological information (size and shape, and then distribution) by visual examination or with a simple microscope; any correlation with surface heterogeneity should be recorded. There are other nondestructive methods (such as X-ray radiography, deflection of electromagnetic or ultrasonic waves around a pit, and penetration of a dye into the pits), which can be used to supplement direct observations of pitting. In the case of highly pitting resistant TiCode-12, however, these methods may not be of much help.

In determining the lifetime of a TiCode-12 container, pit sizes and depths are of foremost importance. ASTM Standard Practice[46] suggests the following categories of methods for pit depth measurements:

- Metallographic - a vertical section is cut through the deepest part of a pit. The pit depth is then measured from the surface to the bottom of the pit with an optical microscope.

- Micrometer or Depth Gauge - a micrometer with a pointed needle, or a depth gauge directly measures the pit depth with respect to the unaffected flat part of the surface. As an alternative, one may use a calibrated microscope and determine the depth by focusing it at the lip and the bottom of the pit.

- Machining - a sample with major faces parallel to each other is used. After pitting exposure and cleaning is over, one of the sample's surface is removed in small steps by parallel machining and the number

of pits at each step counted until all the pits are removed. The difference between two successive steps gives the number of pits with the average depth of that particular step. This method is somewhat tedious but it gives information about the depth distribution as well as maximum pit depth.

To describe the extent of pitting on a surface, ASTM does not recognize any fixed procedure. However, to have a qualitative description, it is useful to describe the pit pattern with reference to ASTM standard chart.[46] To describe susceptibility of pitting of an alloy, a pitting factor defined as the deepest metal penetration/average metal penetration is reported. In TiCode-12 the two penetrations may not be comparable and there can be large uncertainty in the pitting factor.

3.3 System Test

For the final determination of pitting corrosion life of TiCode-12 containers, MCC suggests that the testing be done on a full size container in an environment having as many features of a working repository as practical. Such testing will have to wait until all the details of repository design are completed. Meanwhile, testing should be initiated under laboratory conditions.

3.4 Conclusions

Many of the testing methods discussed above assume that pitting occurs on TiCode-12, even though none of the tests have so far shown[4] any sign of this type of corrosion. Since pitting may have long incubation periods, it is suggested that the tests be continued for periods of up to several years. To induce pitting, the testing should also be done under accelerating conditions (e.g., lower pH, higher temperature, etc. than those expected either in a salt or a basalt repository).

4. TESTS FOR CREVICE CORROSION

4.1 Introduction

Crevice corrosion can occur when stagnant corrosive solution is present in a crevice between the metal and some other surface. In this situation, the metal inside the crevice corrodes in an autocatalytic fashion similar to pitting on an open surface. Most of this type of corrosion can be avoided by minimizing the possibility of a crevice in a properly designed nuclear waste container. However, the container will likely be in contact with backfill or other engineered barriers so that a crevice geometry may be unavoidable. Therefore, the testing of TiCode-12 for crevice corrosion is essential.

Crevice corrosion of commercial titanium in salt solution was shown to be present by Griess[47] many years ago. It was also confirmed that additional small amounts of nickel, molybdenum, or palladium would reduce the alloy's susceptibility to this type of attack. It would then appear that TiCode-12

should be highly resistant to crevice corrosion. In fact, the SNL experiments[6] did not show any sign of crevice corrosion on TiCode-12 in seawater at 300°C. However, recent results from BNL[4,48] have shown significant amounts of crevice corrosion. Assuming a constant rate of corrosion (though unlikely), they found that in 1000 years ~10 cm of metal could be lost inside the crevice. Since there is very little other data available on crevice corrosion of TiCode-12 and this form of corrosion can be a potential failure mode (particularly in salt repositories), extensive testing will be needed to predict the container life.

4.2 Variables Affecting Crevice Corrosion

Oldfield and Sutton[49] have listed most of the relevant parameters which influence crevice corrosion (Figure 7). With reference to TiCode-12 under repository conditions, we may add to this list radiation from the waste form, and lithostatic pressure. Traditionally, most crevice corrosion testing has been performed on steels where a crevice is associated with the presence of chloride or some other halide ion.[50,51] For similar reasons, crevice corrosion on TiCode-12 will likely be more severe in a salt repository than under basaltic conditions. Naturally, in the initial stages, the testing should be done in brines.

Among the factors shown in Figure 7 to affect crevice corrosion, except for temperature (and radiation), all are fixed by the properties of TiCode-12 and the repository. The temperature depends on waste loading conditions.

4.3 Test Methods

From the point of view of basic mechanisms, crevice corrosion is very similar to pitting corrosion. In fact, pitting may be considered as crevice corrosion in which the pit is a self-induced crevice. It has been stated[52] that if an alloy is susceptible to pitting, it will also show crevice corrosion; though the converse may not be true. Due to this similarity, the electrochemical tests described in the last chapter to understand the mechanism of pitting can usually be used for crevice corrosion. However, because of large differences in the physical nature of a pit and a crevice, direct tests for crevice corrosion are distinct and will be discussed next. The electrochemical tests will be discussed only to the extent that they are different from those for pitting.

4.3.1 Direct Tests

As with uniform and pitting corrosion tests, one can expose a TiCode-12 crevice sample to simulated repository conditions, and then examine the material loss either by weight change or some other methods discussed in the previous two sections. However, considering that TiCode-12 is highly corrosion resistant, and did not show crevice corrosion in SNL experiments,[6] it may become necessary to do the testing under accelerating conditions. This is desirable especially because a crevice may have a long incubation period before it starts actively corroding. From the results of Griess,[47] it is

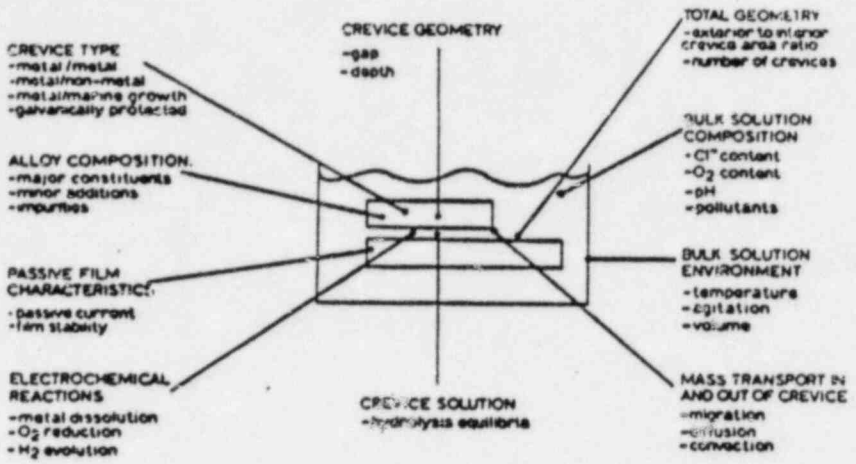

Figure 7. Factors affecting crevice corrosion.[49]

suggested that of the several variables listed in Figure 7, temperature, pH, and Cl^- concentration will be most effective for accelerating the corrosion. However, one should be cautious because in some instances, low pH and high Cl^- variables may not necessarily mean an increase in crevice corrosion.[53]

To test for crevice corrosion in the laboratory, an artificial crevice can be made either between two pieces of TiCode-12 or one piece of TiCode-12 and another inactive material. It is known[72] that different surfaces can nucleate a crevice with varying degrees of effectiveness. In a repository, TiCode-12 will be most likely in contact with the backfill material, which may enhance crevice corrosion. It is difficult, however, to predict the effect the backfill will have. In initial experiments, TiCode-12/TiCode-12 crevices may be used to scope the problem.

In the absence of any fundamental restrictions on crevice geometry, there have been virtually as many kinds of crevices as there are crevice corrosion investigations.[54-58] For the sake of illustration, some crevice configurations are shown in Figure 8. A common deficiency in most of the crevices is the lack of description of its actual width or area. This has caused poor reproducibility even in determining if crevice corrosion exists under the "same" experimental conditions[47] and suggestions are made to include statistical analysis of the scatter in data. Therefore, in the methods not having a crevice with well defined area and width, an experiment should be performed on multiple similar samples and the range of results recorded. Figure 8(b) shows a crevice design which is purported to give reproducible crevice geometry. The France-Greene assembly (Figure 8(c)) has an added feature that potential can be measured along the length of the crevice. Many of the crevice designs referenced here may have the limitation that they cannot be used at temperatures as high as expected in a repository and may require certain modifications.

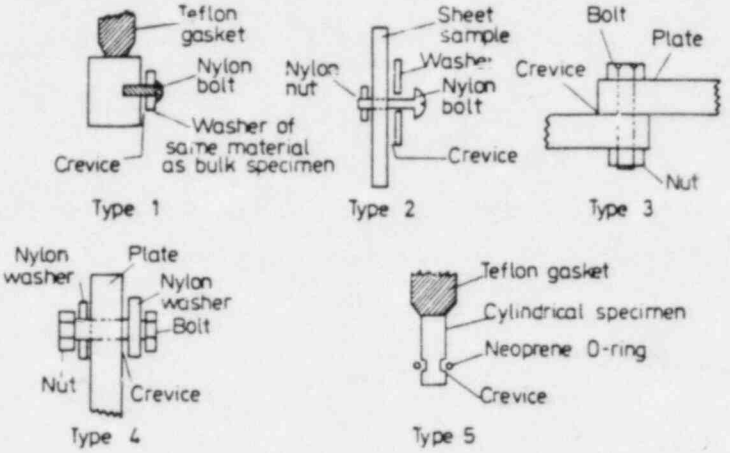

(Taken from Reference 55.)

(a)

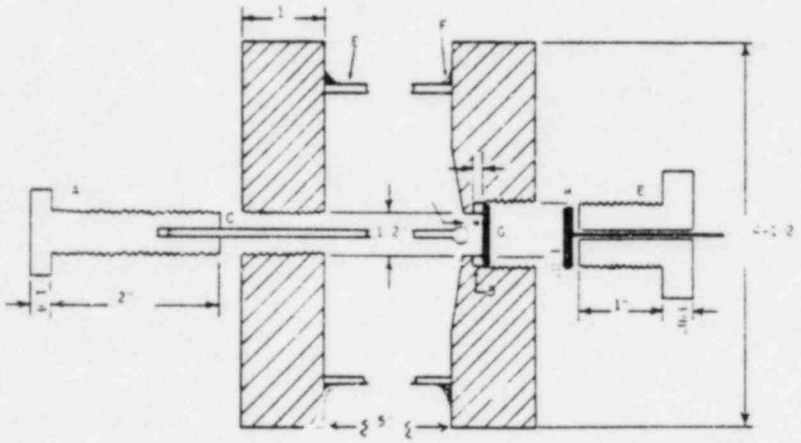

Taken from Lizlovs[57]

A. Teflon bolt
B. PVC bolt
C. Glass rod with glass bead at the end
D. Teflon gasket
E. Glass tubing
F. Silicone rubber mount
G. Stainless steel working electrode
H. Copper disk with copper lead wire.

(b)

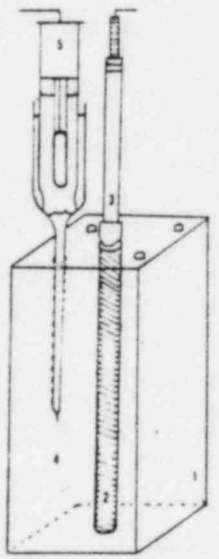

Taken from France and Greene[58]

1. Plexiglass block
2. Specimen
3. Electrode holder
4. Potential probe
5. Saturated calomel reference.

(c)

Figure 8. Various types of crevices used for investigating crevice corrosion.

All the crevice designs mentioned above form a closed system in which the corrosion can be observed only by interrupting the test and dismantling the specimen. In these designs, the crevice region corrodes anodically, whereas the outside surface acts as a cathode. Lee[59] has separated the anodic and cathodic areas by enclosing a small thin sheet specimen between two transparent acrylic blocks and then electrically connecting it to a freely exposed, much larger piece of the same metal. When the whole assembly is exposed to the corroding atmosphere, the small piece along with plastic blocks represents the inside of the crevice and the big piece acts as a cathode. In this way, he could observe the crevice corrosion in situ and get a better understanding of the mechanisms.

To investigate the severity of crevice corrosion, one can measure either the loss in weight or the thickness of the sample. To convert weight loss into a corrosion rate, one would need to know the area of the effective crevice. Then, it will be necessary to make an assumption that all the affected area corrodes at the same rate. Considering recent results on TiCode-12, which show a corrosion gradient within the crevice, this assumption may need careful evaluation. In thickness measurements, one may prefer to determine the maximum rather than the average reduction in thickness, using one of the methods described in the last section on pitting.

4.3.2 Electrochemical Tests

Crevice corrosion is usually considered to proceed in four stages: (1) consumption of oxygen within the crevice without any refurbishing from outside, thus, an oxygen concentration cell is formed, (2) increase in acidity and chloride concentration within the crevice, (3) breakdown of the oxide passivation film and initiation of fast corrosion, and (4) propagation of crevice corrosion. By simply observing the crevice, one can identify the third and fourth stages of corrosion and correlate them with large changes in current. In this way, the incubation time and the time of rapid corrosion are known individually. With this information, the rate of crevice corrosion can be calculated more accurately rather than by simple averaging over the total test period; the error can be substantial in alloys having long incubation periods.

In the open crevice configuration[59] described earlier (also see Reference 56), a zero impedance ammeter is connected between the cathode and anode. Thus, the current between the cathode and anode may be monitored continuously as crevice corrosion proceeds. This current may be a good measure of corrosion, since its correlation with direct weight loss was observed for stainless steels in seawater. This method of testing is not an electrochemical type in the sense it is described in earlier sections, but it can provide information about the corrosion mechanisms. As for the corrosion current, the corrosion potential (E_{corr}) shows large changes (Figure 9) during breakdown of passivity. Therefore, measurements of E_{corr}[53] can also be used to determine the beginning of rapid crevice corrosion. Note that all the events of micropitting and coalescing of pits shown in Figure 9 are specifically for Type 316 stainless steel, and may not be visible on

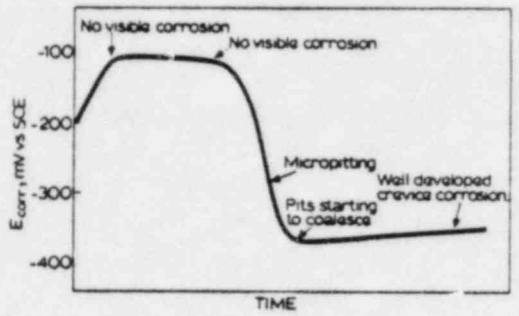

Figure 9. Schematic composite E_{corr}/time curve showing the development of corrosion of Type 316 stainless steel crevices.[53]

TiCode-12. Although E_{corr} shows time variation for different stages of crevice corrosion, the corrosion current can give quantitative data on corrosion rates as well.

The basic idea behind ordinary potentiostatic (dynamic) or galvanostatic (dynamic) testing for crevice corrosion is the same as for pitting described in the previous section. Therefore, we shall examine only new considerations which are specially relevant to crevice corrosion. For the given corrosion conditions, a generally referred electrochemical parameter is the protection potential below which a pit or crevice will repassivate. However, values of this potential may depend to some extent on the method of measurement and hence it may not be a unique quantity. Wilde[60] has compared his cyclic potentiodynamic results on stainless steel samples having artificial crevice, with long term direct weight loss measurements. He concludes that the severity of crevice corrosion in an alloy increases with the area of the hysteresis loop on the voltage vs log (current) cyclic curve. This is an important observation in quantifying crevice corrosion of TiCode-12 under varying conditions. However, it must be realized that Wilde's conclusion is based on empirical observations. Therefore, it needs to be shown that TiCode-12 also obeys such an empirical formulation.

In spite of the close similarity between pitting and crevice corrosion, there are some obvious differences. Crevice corrosion occurs in a small closed volume whose characteristics can be changed much more readily than those of pitting which will probably occur on a much larger area. Thus, within a pit while the local chemistry may be substantially different, it is well exposed to the rest of the solution. As a result, the kinetics and probably some details of the mechanisms of pitting and crevice corrosion can be substantially different. Therefore, when making any potential measurements, it will be desirable, to differentiate between pitting and crevice corrosion. Garner[61] found for stainless steels, that in a potentiostatic study after applying a temporary voltage more positive than the pitting potential, the decay characteristics of the open circuit potential depended on whether pit-

ting or crevice corrosion had been initiated. Depending on whether the steady state potential was in active or passive region, the presence or absence of crevice corrosion could be determined. It cannot be predicted if similar observations will be found for TiCode-12, but studies of potential-time transients may be a helpful and simple means of evaluation.

Since a crevice (at least the ones prepared artificially) is much larger than a pit, the conditions of corrosion within a crevice can be studied more easily. An important parameter concerning crevice corrosion is the actual pH of solution within the crevice at which corosion starts, since this information can be used to conduct further tests in an open solution at this pH. Griess[47] measured in situ pH in a titanium crevice at 150°C (in an autoclave) by withdrawing a very small volume (~.05 ml) of crevice solution. To do this, he had welded a titanium capilliary to the center of the crevice, passing through the head of the autoclave.

Some observations from Griess' study[47] on titanium and its alloys are very relevant for the testing of TiCode-12:

1. He determined the changes in pressure and composition of autoclave gases. In this way, he could determine what fractions of oxygen reduction and formation of hydrogen reactions were responsible for the cathodic half of the electrochemical reaction.

2. In principle, it is considered that a metal can be brought to an active state by the application of a proper external potential. However, Griess could not induce an active state by either cathodic or anodic polarization in a solution in which crevice corrosion occurred. He then suggested that an active crevice must have an acid concentration greater than 10^{-3} M.

3. Highly cathodic polarization produced hydride on the surface, which soon decomposed reforming a metallic surface.

4. Generally, it is difficult to clean the oxide film from the surface of titanium and its alloys. To obtain an anodic polarization curve in acidified brine, the solution was deoxygenated and the metal was pickled lightly in an HNO_3-HF solution.

5. The relative degree of resistance of titanium (and hence very likely TiCode-12) to acid chloride solutions to be found in a crevice could be determined from anodic polarization curves at temperatures below which crevice corrosion is a major problem.

6. Finally, the activity of hydrogen ions, rather than the concentration, determined the rate of attack. Actually, the anion associated with acid was of little importance as long as acidity existed. The activity coefficient of hydrogen increases as the concentration of sodium chloride in solution increases. Thus indirectly, composition of brine or groundwater is an important parameter in influencing the rate of crevice corrosion.

4.3.3 Other Measurements

Since the occurrence of crevice corrosion in TiCode-12 was demonstrated only recently, this form of corrosion has hardly been characterized. Therefore, along with any direct or electrochemical testing on TiCode-12, materials characterization techniques such as optical and electron microscope, microprobe, X-ray diffraction, etc. should be used to obtain supplementary information. This approach at BNL[48] has shown the presence of some lower oxides of titanium and that there is a potential/chemical gradient within the crevice. Thus, it may not be appropriate to treat a crevice as a homogeneous entity. Confirmatory experiments will be desirable for a spatially uniform crevice such as shown in Figure 8(b). Some other questions concerning the effect of surface oxide layers on crevice corrosion were raised, which may be answered by correlating surface studies with cathodic polarization behavior.

Concentration of dissolved oxygen is an important consideration because the initial stage of crevice corrosion involves depletion of oxygen. Hence, the larger the amount of dissolved oxygen, the longer it should take for crevice corrosion to occur. In relation to crevice corrosion in a repository, it may be noted that due to radiolysis, concentration of dissolved oxygen may be considerably affected. When oxygen or some other oxidizing agent is one of the radiolysis products, it is possible that the crevice is continuously buffered by them, thus delaying the initiation of crevice corrosion. The details of this possibility are discussed by Lee.[2] Testing under irradiation will be necessary to evaluate this aspect of crevice corrosion of TiCode-12.

4.4 Conclusions

Crevice corrosion of TiCode-12 under simulated repository conditions has been recently shown[48] to occur and hence is a potential mode of container failure. Whereas relatively extensive testing of TiCode-12 has been performed on uniform corrosion, crevice attack has not been adequately addressed. Therefore, from the standpoint of the life of a TiCode-12 container, extensive testing on crevice corrosion is required under realistic conditions.

Generally, depletion of oxygen from the crevice may be considered a prerequisite for the initiation of corrosion. Under radiation conditions some oxidizing agents may be produced by radiolysis within the crevice and hence delay the onset of corrosion. On the other hand, radiolysis might lower the solution pH and hence expedite crevice attack. At a later stage, or in some areas where effective radiolysis is negligible, crevice corrosion may occur early. Thus, testing needs to be performed under both conditions.

Finally, high concentrations of anions (mostly Cl^-) and temperature and low pH are expected to accelerate crevice corrosion, and may be used to reduce the incubation time for initiation of rapid crevice corrosion. Testing as a function of these parameters both by direct as well as electrochemical methods will be useful. As these tests proceed, an input should be obtained from other materials characterization techniques to determine further testing requirements.

5. TESTS FOR HYDROGEN EMBRITTLEMENT

5.1 Introduction

Titanium and its alloys are known to show considerable degradation in their mechanical properties in the presence of hydrogen. In TiCode-12, 30-50 ppm hydrogen is normally present after the manufacturing process and large additional amounts can be absorbed when the container is exposed to radiolysis products in the repository. Even small concentrations of hydrogen may cause failure in a stressed container so that testing for hydrogen embrittlement failure modes is mandatory.

The general area of hydrogen embrittlement covers a very large volume of scientific research including a variety of testing methods. Figure 10 (taken from Reference 62) describes a model for hydrogen interaction with an alloy. When hydrogen enters from an outside environment, the interaction on the surface will play an important role. For example, on TiCode-12 having an oxide film, the oxide may act as a barrier for hydrogen penetration into the metal.[63,64] However, it is possible that in some areas the oxide film is broken or dissolved (as in a crevice) and the oxide-free alloy surface may readily absorb hydrogen or form a hydride if the hydrogen concentration is sufficiently high. The hydride can continue to supply hydrogen via diffusion into the bulk even after its primary source has ceased to operate. Also, specimen texture, exposure, atmosphere, and preparation techniques can change the oxide characteristics and hence the hydrogen uptake rate. Hydrogen present from mill processes will diffuse easily within the structure, probably at a faster rate along the grain boundaries.

Unlike iron-based alloys, the embrittlement of a titanium alloy occurs primarily due to the formation of a hydride phase within the matrix; other mechanisms shown in Figure 10 are of minor importance. A stress pattern, such as triaxial stresses in the container may serve as a driving force for hydrogen to diffuse from the bulk and concentrate locally around metallurgical imperfections. Thus, a hydride phase may be formed when the local concentration of hydrogen exceeds the solubility limit. Since diffusion is a time dependent phenonenon, the embrittlement of TiCode-12 due to the hydride phase will also be time dependent and can have a long incubation period depending on temperature, stresses, and the concentration of hydrogen. This makes it hard to predict the long term effects of hydrogen on the mechanical properties of TiCode-12. Also, small concentrations of hydrogen which may seem to be unimportant from short term laboratory tests, can cause embrittlement after extended periods due to the problem of delayed fracture. Therefore, a conservative approach in testing the mechanical properties and subsequent design parameters of the TiCode-12 container is warranted.

The presence of significant quantities of hydrogen in TiCode-12 or in the surrounding environment may be deleterious with respect to delayed failure and brittle fracture. Therefore, any measurement technique[65] which evaluates these two effects will provide relevant information. Different testing

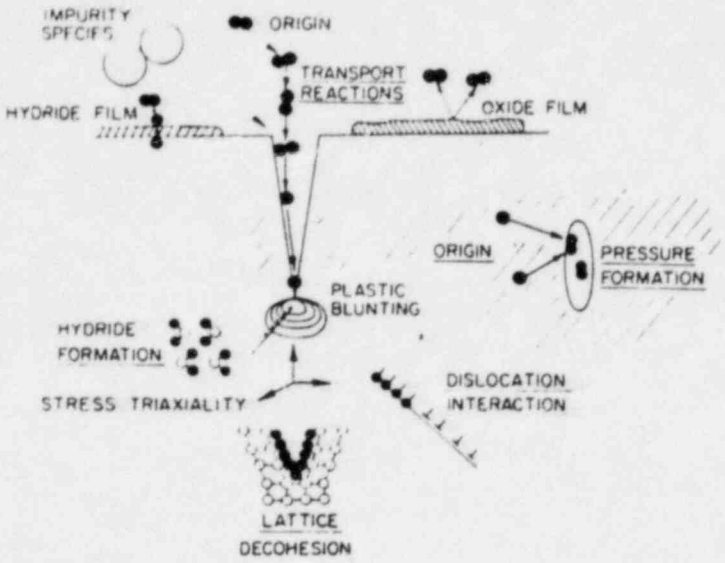

Figure 10. Interaction of hydrogen with an alloy.[62]

techniques have varying ability to quantify hydrogen embrittlement effects (see Figure 11).[66] Simple techniques such as disk pressuring[67,68] or the measurement of reduction in area are sufficient to demonstrate whether a given material is susceptible to adverse effects of hydrogen. However, the data obtained from these methods may be of limited importance in determining the performance of the TiCode-12 container. On the other hand, the technique of fracture mechanics is expected to yield quantitative data which can be used in evaluating the failure of TiCode-12. Accordingly, in its summary report,[16] the MCC Workshop has recommended static and dynamic fracture mechanics tests to quantify the hydrogen effects. The present report will mostly address these tests.

5.2 Variables Affecting Hydrogen Embrittlement

The main concern from the presence of hydrogen is that a TiCode-12 container might fracture during the containment period even though the applied load is much less than its ultimate strength. Archbold and others[69,70] have discussed in detail the hydrogen effects related to failure of titanium and its alloys (not TiCode-12 in particular) and have identified the following factors which determine the kinetics of cracking:

- Concentration of hydrogen with respect to the solubility limit - this limit itself will be determined by the temperature, stresses, microstructure, etc. The larger the content of hydrogen above the solubility limit at a given temperature, the faster will be the formation of hydrides and embrittlement.

- Absorption of hydrogen from environment - radiolysis of water will continuously produce hydrogen which can be absorbed by the container.

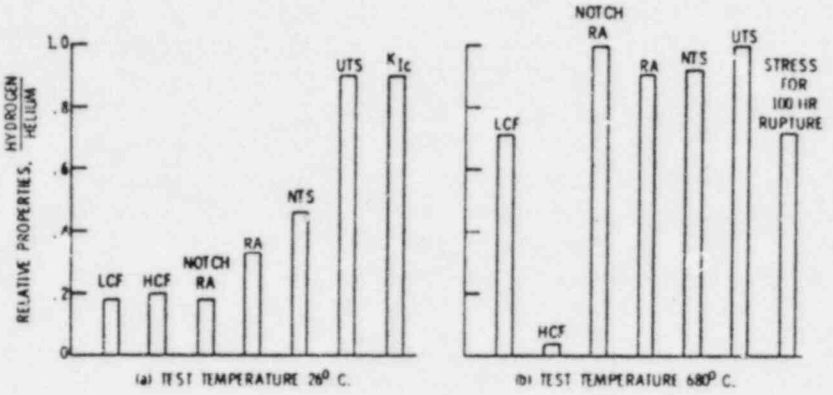

Figure 11. Comparison of mechanical properties of Inconnel 718 determined in hydrogen and helium at a pressure of 35 MN/m^2 (5000 psi).[66] Alloy annealed at 1038°C; notched specimens, K_t = 8; LCF, 1 to 2% strain; HCF, R = 0.1, (a) 180 ksi, (b) 140 ksi.

The production rate of hydrogen will depend on the intensity of irradiation and the chemistry of the groundwater. The hydrogen absorption rate will depend upon the container-surface conditions. When the radiolysis produces atomic hydrogen at the surface, it will probably enter the alloy more readily than molecular hydrogen gas. This fact should be kept in mind for laboratory tests simulating repository conditions.

- Strain rate in comparison with the diffusivity of hydrogen - in general a slower strain rate gives more time for hydrogen diffusion and hence more pronounced embrittlement. However, when hydrogen diffusion is not the rate determining step, the stain rate dependence will become less important. Some titanium alloys have shown[71] increased embrittlement at very high strain rates as a consequence of the strain rate sensitivity of the flow and fracture stresses of titanium hydrides rather than the metal itself.

- Internal flaws, cracks and stresses - the flaws and cracks present from the production process may not be easy to control and may enhance the embrittlement. Therefore, in this respect the test specimens should be representative of the final container material. Residual stresses resulting from the fabrication procedure including any welding should be taken into consideration during testing.

- Temperature - this variable affects both the solubility limit as well as the diffusivity of hydrogen. Therefore, its effect on embrittlement is not easy to predict, and testing should be carried out over the temperature range expected in a repository.

- Microstructure - TiCode-12 is a near-alpha titanium alloy. It has a small amount of beta-phase presumably present as a continuous network along the grain boundaries[9]. The beta-phase has higher hydrogen solubility and low susceptibility for hydride formation[2,73], and therefore is less susceptible to hydrogen embrittlement. Depending on the concentration of hydrogen, the fracture of TiCode-12 occurs at alpha-beta boundaries or through alpha grains[20]. In short, as shown for commercially pure titanium[74], the phase morphology, grain size, properties of the grain boundary etc. are important parameters. Hence microstructural analysis should be included for all embrittlement testing. Any preferred orientation appearing in the actual container should also be given due consideration. Welding of the container is likely to change the microstructure in the heat affected zone. Therefore, separate testing of welded specimens will be needed.

- Irradiation - the direct effect of this variable on hydrogen embrittlement is not known, but it is likely that the radiation can help in the formation of the hydride phase.

Fatigue cracking due to cyclic loading and stress corrosion cracking are other important aspects of hydrogen embrittlement testing. However, cyclic loading is not expected in a repository and should not be of great importance except as an accelerating test. Stress corrosion cracking is considered to be a serious mode of failure and has been discussed elsewhere in a separate report.[75]

5.3 Accelerated Testing

From the available information on the hydrogen effects in titanium and its alloys,[2] it is evident that the amount of hydrogen present in a commercial TiCode-12 sample may be too low to show significant embrittling effects within the laboratory time scale. However, it is difficult to assert that such small concentrations can be ignored for the repository time scale. Additional amounts of hydrogen may also be absorbed by the alloy during radiolysis[76] of the groundwater. Clearly, the laboratory testing conditions need to be made more severe to accelerate the embrittlement mechanism. In the case of corrosion failure discussed in the previous sections, testing could be accelerated by increasing the temperature or lowering the solution pH. Since hydrogen embrittlement is known to be a low-to-moderate temperature range phenomenon, increasing the test temperature will not necessarily accelerate it. The effect of pH falls under the category of stress corrosion cracking, and is discussed elsewhere in this study. Increasing the concentration of hydrogen will expedite the embrittling process and hence is a natural choice for acceleration purposes.

As for any other test acceleration procedures, one must be cautious in extrapolating the accelerated test data to real situations. Acceleration by increasing the hydrogen concentration can easily change the mechanisms of embrittlement and an extrapolation to lower concentration may not be appropriate. Table 2 shows that the relation of hydrogen concentration with

Table 2

Effect of Hydrogen Concentration on K_{ITh} of Ti-6Al-4V[77]

Hydrogen, ppm by Weight	K_{ITh}* (MPa m)
8	92
36	65
53	67
122	64
215	66

*K_{ITh} is the lowest value at which sustained crack growth occurred.

the threshold stress intensity factor, which is a measure of embrittlement, is not linear. In spite of the ambiguity in extrapolating such results to lower concentrations, it may be noted that in general, the result should be a conservative estimate.

The concentration of hydrogen in an alloy sample can be increased by one of the following three procedures:

1. Heating a test specimen in a suitable hydrogen environment at a higher temperature where the solubility as well as diffusivity is larger - once the specimen has absorbed the desired amount of hydrogen, it can be cooled and tested at lower temperatures. This method is more appropriate for the materials (e.g., TiCode-12 which predominantly comprises alpha phase) which have low diffusivity, and thus cannot have homogeneous distribution of hydrogen at the room temperature. Furthermore, one can control the composition of the charging gas.

2. Cathodically charging the specimen - here, hydrogen from an H^+ containing acidic medium collects on the specimen surface and diffuses in. This method is simpler to use but is not appropriate for thick specimens.

3. Performing the embrittlement test in hydrogen gas - this approach is appropriate for determining hydrogen environmental embrittlement.

5.4 Fracture Toughness Parameters

Fracture toughness is a generic term to describe the resistance to extension of a crack.* Therefore, a parameter is needed to define this property quantitatively using available information from a prescribed testing procedure. This parameter should conform to the conditions expected for a container in a repository, and preferably be easy to determine.

The majority of the fracture toughness tests involve plane strain samples. The resistance of the material to sustained load fracture is then described by the threshold value of the stress intensity factor (K_{Th}) below which a crack will not propagate during a specific time. This parameter has obvious uncertainties of having a lower value if the test time is increased. There may also be some dependence on test specimen design, etc. In spite of some ambiguity, K_{Th} has been extensively used in screening various materials. By correlating plane strain fracture toughness (K_{Ic}) and dynamic tear energy with yield strength, ratio analysis diagrams[78] have been developed and may be used for interpreting the fracture resistance of materials in terms of damage tolerant design. Evaluation of fracture toughness using the threshold parameters has been a widely tested method and hence also better understood. The BNL group has adopted[48] this approach to evaluate the fracture toughness of TiCode-12, and from preliminary experiments determined K_{Th} to be approximately 4.5 MPa $\sqrt{m}$.

A general criticism on the use of K_{Th} as a fracture toughness criterion is that it is applicable only when plane strain conditions of elasticity are valid.[69] Thick compact tension specimens can approximately meet these conditions, but a thin TiCode-12 container probably will not. With the possibility of substantial plastic deformation during testing and use in the repository, a different set of test methods has been suggested,[79] particularly the J-integral and R-curve methods. The J-integral is a mathematical expression and gives the critical parameter J_{Ic} to represent the material toughness at or near the onset of crack extension. A threshold value of J_{Ic} (J_{Th}) is defined analogous to K_{Th} and as long as minimum specimen size requirements are met, it is a specific material property.[80] For materials which fracture in a ductile fashion on a microscale, J_{Th} is expected to give more conservative values for fracture toughness than K_{Th} and hence is a preferred parameter.[81] However, a big disadvantage in determining J_{Ic} is that it involves the measurement of crack growth in a series of experiments, which is a tedious procedure.

The R-curve represents the resistance to fracture during incremental extension of a crack. The crack resistance is described in terms of the stress intensity factor K_R and can be obtained from a variety of tests.[79,82] In principle, R-curve analysis can predict critical fracture stress and flaw size of an untested specimen at instability even when plane strain conditions are not satisfied. However, experimental knowledge of such predictions is very limited and the method is more complex than the determination of K_{Th}.

*A glossary of the commonly used terms in fracture testing is described in the Annual Book of ASTM Standards, Part 10, Designation E616-81.

From the present understanding and reliability in translating the laboratory data of K_{Th}, J_{Th}, and R-curve analysis to actual design, it is suggested that extensive testing on TiCode-12 should be focused on K_{Th} measurements. Some supplemental testing should, however, be carried out to demonstrate that K_{Th} is not too unrealistic compared to the results obtained from J-integral data.

5.5 Test Methods

The MCC Workshop has considered[16] the methods to test hydrogen effects in engineered barrier materials. These are divided into two broad categories: static test methods and dynamic test methods. An experiment may be performed using bend,[79] compact tension,[79] wedge opening load[83] or cantilever beam tests.[83] Some details of these tests are described in a separate report.[75]

The C-type and U-bend tests considered appropriate for stress corrosion cracking (SCC)[75] are, however, not recommended for hydrogen embrittlement due to lack of triaxial stress conditions. Among the suggested test methods, some are easy to use but appropriate for screening of available materials. Having selected TiCode-12 as the container material, such tests will not be necessary. Then, the MCC recommended tests will be as mentioned in the sections below.

5.5.1 Static Test Methods

These methods include:

- Slow crack growth using a fixed load on compact tension specimens. Determine K_{Th} or J_{Th}.
- Slow strain rate using compact tension specimens. Determine K_{Th} or J_{Th}.
- Same procedure as in the previous two tests, but on center cracked sheet specimens. This method may be useful for determining texture effects. Also, a logitudinally cracked tube can instead be used under load control for the same purpose.

In general, these methods use a specimen which has been previously fatigue cracked to provide stress intensification in a reproducible manner; a short fatigue crack extends from a notch machined in the specimen. The relative length of the crack, the dimensions of the notch and the specimen, and the procedure to produce a fatigue crack are prescribed by ASTM.[84] In some cases, if crack initiation and growth require an excessive number of fatigue cycles, ASTM recommends using a very sharp notch tip, statically pre-loading the specimen in such a way that the notch tip is compressed in a direction normal to the intended crack plane, or using a chevron notch.

To determine K_{Th}, one needs to find out the value of plane strain fracture toughness K_{Ic} below which there is no observable crack growth. ASTM has set a standard test method[86] for the determination of K_{Ic}. For

the determination of both K_{Th} or J_{Th}, an important step is to measure the crack length under different conditions. There are a variety of methods which yield directly or indirectly the value of crack length as it grows. These are summarized by Deaus and others[85] and listed in Appendix A.

A test not mentioned in ASTM procedure or MCC recommendations uses a double cantilever beam specimen and is recommended by Archbold and others[70] as a predictive test for monitoring and predicting delayed failure due to hydrogen embrittlement as well as SCC. This technique has been used by Boyer and Spurr[87] with the specimen configuration shown in Figure 12.

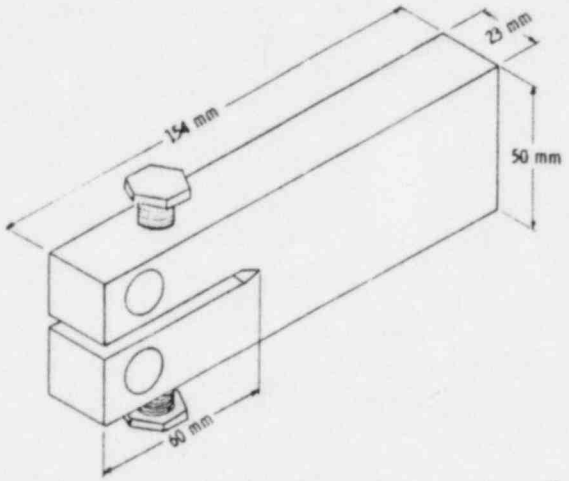

Figure 12. Specimen for double cantilever beam technique.[87]

The specimens are fatigue pre-cracked and loaded to desired stress levels in an Instron machine before starting to measure the crack growth. Here, the value of stress intensity decreases as the crack length increases. This method has the advantage of relatively low cost specimens which can be easily used under various conditions. Furthermore, an Instron machine is needed only to pre-load the specimen and subsequent loading is maintained by the bolts. Several specimens can be tested concurrently. This will, however, not permit any variation in strain rate as it affects the crack growth. For Ti-6Al-4V alloy, this method was found to be useful to detect texture related effects.[87]

The MCC recommended test when plane strain conditions are not present is the determination of threshold value of J-integral which is defined[88] by:

$$J = [W\,dy - T\cdot(\partial\bar{u}/\partial x)]\,ds$$

where:

W = Loading work per unit volume, or for elastic bodies, strain energy density
x,y,z = Rectangular coordinates

ds = Increment of the contour path
T = Outward traction vector on ds
$\bar{u}$ = Displacement vector at ds
$T \cdot (\partial u/\partial x)ds$ = The rate of work input from the stress field into the area enclosed by Γ, the path of the integral which contains the crack tip.

The standard method for determining J_{Ic} which is the value of J at crack initiation is described in the ASTM manual.[88] Here the purpose is to obtain load vs crack displacement curve by loading the specimen to different displacement values in a series of tests. The displacement at each step may be measured by heat tinting the specimen. Clarke and others[89] have developed a fully autographic method to determine J_{Ic} using one specimen and periodic partial unloading. In this case, the reciprocal of the unloading slopes (in load vs load time displacement plot) normalized for elastic modulus and specimen geometry, predict the crack size using an elastic compliance calibration.

R-curve determination is another approach to evaluate the resistance to fracture during incremental slow crack extension from a sharp notch. MCC has not considered this method as best suited for the design of waste containers; nevertheless, it is a relevant test and its details are described in the ASTM manual.[82]

In any of the test methods using thick specimens, one should be cautious of any errors due to "tunneling". This happens when the crack front penetrates deeper in the middle of the sample than on the surface. Thus, crack growth conditions may become more severe in the interior of the specimen and lead to a failure, while the observations from the surface give erroneous results.

5.5.2 Dynamic Test Methods

Except for the applied load, dynamic tests use the same kind of specimen, data analyses, etc. as do the static methods. Here, a cyclic stress is applied whose intensity varies between a minimum (e.g., zero) and a maximum value (K_{max}) at a frequency <30 Hz. The results may be expressed in terms of ΔK_{Th} below which the material will not fail irrespective of the total number of cycles. In general, this parameter will give more conservative estimate of fracture toughness of a material, otherwise each dynamic method has the same advantages or disadvantages as the corresponding static method.

5.5.3 Weld Tests

It was mentioned earlier that due to the changes in microstructure or additional stresses, the area around a weld may be more susceptible to hydrogen embrittlement and fail earlier than the rest of the container. This adverse effect may also deteriorate toughness and SCC resistance of TiCode-12. A general description of specimen preparation, welding configuration and testing method is given in the ASTM manual.[17] To evaluate the potential of

hydrogen assisted delayed cracking, a weld bead is prepared[90] between a helically notched cylindrical TiCode-12 test specimen after inserting it into a plate of the same material. The stress intensification for hydrogen diffusion is provided by the notch and the welded structure is tested in a static mode. Toughness of the weld may be determined by having a notched specimen and stressing it in a bending mode. Charpy V-notch tensile tests will also give information about toughness. Weymueller[91] has discussed the merits of these tests.

An as-welded TiCode-12 component may have developed strong internal stresses due to inhomogeneous cooling. These stresses can considerably decrease the life of the container and may lead to early failure. Important methods to measure internal stresses are listed by Archbold and Polonis.[69] Since the present goal is not to characterize internal stresses but to evaluate their adverse effect on the container performance, these test methods may not be necessary. Previously described hydrogen embrittlement tests performed on welded specimens will include the effects of internal stresses also. However, if internal stresses become a major concern of failure, proper annealing treatment after welding should be considered to relieve them. This may improve ductility and toughness of the welded zone.[92]

5.6 Conclusions

Hydrogen in TiCode-12, present internally from manufacturing processes or absorbed during repository exposure, is likely to deteriorate mechanical properties of the container to the extent that hydrogen embrittlement is a potential failure mode. The most important property of concern is the crack growth under sustained load conditions. Fracture mechanics tests are considered to be appropriate to evaluate hydrogen effects.

Due to possible small hydrogen concentrations in as-received specimens, accelerated testing will be needed. Temperature, strain rate, microstructure, irradiation, etc. may influence the extent of the effect of hydrogen on the mechanical properties of TiCode-12, but their dependence may not be monotonic and difficult to determine. Therefore, to accelerate the testing procedure, the specimens may be charged with additional hydrogen from an outside source. Several experiments will be needed to be able to extrapolate laboratory data to expected hydrogen contents in the repository.

The determination of K_{Th} or ΔK_{Th} for plane strain conditions is an appropriate starting point to evaluate the hydrogen effects. Some experiments to determine J_{Th} will be useful in determining how much difference it will make if elastic-plastic conditions are present. The double cantilever beam test[87] is also an attractive test method especially when many specimens need to be tested with a limited number of testing machines.

6. REFERENCES

1. R. Dayal, B. S. Lee, R. J. Wilke, K. J. Swyler, P. Soo, T. M. Ahn, N. S. McIntyre and E. Veakis, "Nuclear Waste Management Technical Support in the Development of Nuclear Waste Form Criteria for the NRC," NUREG/CR-2333, Vol. 1 (1982).

2. "Waste Package Data Requirements for TiCode-12 to Show Compliance with 1000-year Containment Criterion," BNL-NUREG Reports under FIN-A-3164. In preparation (1982).

3. B. Siskind and D. Hsieh, "Near-Field Repository Conditions in Basalt and Salt," NUREG/CR-2780, Part 1, BNL-NUREG-51548, May 1982.

4. J. Shao and P. Soo, " Uniform and Pitting Corrosion Data Requirements for TiCode-12 High Level Waste Containers," NUREG/CR-2769, Part 2, BNL-NUREG-51548, May 1982.

5. W. E. Berry, "Testing Nuclear Materials in Aqueous Environments," Handbook of Corrosion Testing, W. H. Ailor, Ed. (John Wiley and Sons, 1971), Chap. 13.

6. W. J. Anderson, "Corrosion Tests of Canister and Overpack Materials in Simulated Basalt Groundwater," Rockwell Hanford Operations, RHO-BWI-ST-15, May 1981.

7. S. G. Pitman, B. Griggs and R. P. Elmore, "Evaluation of Metallic Materials for Use in Engineered Barrier Systems," Scientific Basis for Nuclear Waste Management, Vol. 3, J. G. Moore, Ed. (Plenum Press, 1981).

8. R. J. Hart, "Testing in Hot Brine Loops," Handbook of Corrosion Testing, W. H. Ailor, Ed. (John Wiley and Sons, 1971), Chap. 12.

9. T. M. Ahn and P. Soo, "Container Assessment - Corrosion Study of HLW Container Materials," NUREG/CR-2317, Vol. 1, No. 3, BNL-NUREG-51449, January, 1982.

10. J. W. Braithwaite, N. T. Magnani and T. W. Mumford, "Titanium Alloy Corrosion in Nuclear Waste Environments," SAND-79-2023c (1979).

11. S. D. Cramer and J. P. Carter, "Laboratory Corrosion Studies in Low and High Salinity Geobrines of the Imperial Valley," Bureau of Mines Rept. PB81-104564 (1980).

12. J. W. Braithwaite and M. A. Molecke, "Nuclear Waste Canister Corrosion Studies Pertinent to Geologic Isolation," Nuc. and Chem. Waste Management, 1, 37 (1980).

13. D. B. Stewart and R. W. Potter II, "Application of Physical Chemistry of Fluids in Rock Salt at Elevated Temperature and Pressure to Repositories for Radioactive Waste," U. S. Geological Survey, Scientific Basis for Nuclear Waste Management, Vol. 1, 1978.

14. G. E. Raines, L. O. Rickertson, H. C. Claiborne, J. L. McElroy and R. W. Lynch, "Development of Reference Conditions for Geologic Repositories for Nuclear Waste in the USA," SAND-80-2416c (1980).

15. K. J. Swyler, R. W. Klaffky and P. W. Levy, "Recent Studies on Radiation Damage Formation in Synthetic NaCl and Natural Rock Salt for Radioactive Waste Disposal Applications," Scientific Basis for Radioactive Waste Management, Vol. 2, C. J. Northrop Jr., Ed. (Plenum Press, 1980).

16. M. D. Merz, G. E. Zima, R. H. Jones and R. E. Westerman, "Workshop on Corrosion of Engineered Barriers, Summary Report," PNL-3720, March 1981.

17. "Preparation of Stress Corrosion Test Specimens for Weldments," Annual Book of ASTM Standards, Part 10, Designation G58-78, 1981.

18. "Standard Practice for Preparing, Cleaning and Evaluating Corrosion Test Specimens," Ann. Book of ASTM Standards, Part 10, Designation G1-81, 1981.

19. R. E. Westerman, "Investigation of Metallic, Ceramic, and Polymeric Materials for Engineered Barrier Applications in Nuclear Waste Package," PNL-3484 (1980).

20. T. M. Ahn and P. Soo, "Container Assessment - Corrosion Study of HLW Container Materials," NUREG/CR-2317, Vol. 1, No. 4, BNL-NUREG-51449, April, 1982.

21. L. Callow, J. Richardson and J. Dawson, "Corrosion Monitoring Using Polarisation Resistance Measurements, Part I and II," Brit. Corr. J., 11, 123 (1976).

22. M. J. Danielson, "Application of Linear Polarization Techniques to the Measurement of Corrosion Rates in Geothermal Brines," Geothermal Scaling and Corrosion, ASTM STP 717, 41 (1980).

23. I. Epelboin, C. Gabrielli, M. Keddam and H. Takenouti, "A. C. Impedance Measurement Applied to Corrosion Studies and Corrosion Rate Determination," Electrochemical Corrosion Testing, ASTM STP 727, 150 (1981).

24. S. Haruyama and T. Tsuru, "A Corrosion Monitor Based on Impedance Method," Electrochemical Corrosion Testing, ASTM STP 727, 167 (1981).

25. R. W. Schutz and L. C. Covington, "Effect of Oxide Films on the Corrosion Resistance of Titanium," Corrosion, 37, 585 (1981).

26. "Conventions Applicable to Electrochemical Measurements in Corrosion Testing," and "Method for Making Potentiostatic and Potentiodynamic Anodic Polarization Measurements," Ann. Book of ASTM Standards, Part 10, Designation G3 and G5 respectively, 1981.

27. D. de G. Jones and M. G. Masterson, "Techniques for the Measurement of Electrode Processes at Temperatures Above 100°C," Advances in Corrosion Sci. Tech., Vol. 1, M. G. Fontana and R. W. Staehle, Eds. (Plenum Press, 1970).

28. D. D. MacDonald, B. C. Syrett and S. S. Wing, "The Use of Potential - pH Diagrams for the Interpretation of Corrosion Phenomena in High Salinity Geothermal Brines," Corrosion, 35, 1 (1979).

29. B. C. Syrett, D. D. MacDonald and H. Shih, "Pitting Resistance of Engineering Materials in Geothermal Brines," Corrosion, 36, 131 (1980).

30. O. P. Arora and J. P. Gudas, "Potentiostatic - Ellipsometric Studies of Titanium - Aluminum Binary Alloys in 3.5% Sodium Chloride Solution," NAVSHIPRANDLAB Rept. 8-730, April 1971. AD725504.

31. E. J. Gumbel, "Statistics of Extremes," Columbia University Press, 1958.

32. H. F. Finley, "An Extreme Value Statistical Analysis of Maximum Pit Depths and Time to First Perforation," Corrosion, 23, 83 (1967).

33. Y. Ishikawa, T. Ozaki, N. Hosaka and O. Nishida, "Pitting Corrosion Life Prediction of Machine Components by Means of Extreme Value Statistical Analysis," in Environmental Degradation of Engineering Materials in Aggressive Environments, Proceedings of Second International Conference on Environmental Degradation of Engineering Materials, September 21-23, 1981, Virginia Polytechnic Institute, Blacksburg, VA.

34. T. R. Beck and S. G. Chan, "Experiemntal Observation Analysis of Hydrothermal Effects on Growth of Small Pits," Corrosion, 37, 665 (1981).

35. F. A. Posey and E. G. Bohlmann, "Pitting of Titanium Alloys in Saline Water," Desalination, 3, 269 (1967).

36. Electrochemical Techniques for Corrosion, (National Assoc. Corrosion Engineers 1977).

37. N. D. Greene and M. G. Fontana, "An Electrochemical Study of Pitting Corrosion in Stainless Steels," Corrosion, 15, 32t (1959).

38. S. W. Dear, Jr., W. D. France, Jr., and S. J. Ketcham, "ELectrochemical Methods," Handbook of Corrosion Testing and Evaluation, W. H. Ailor, Ed. (John Wiley and Sons, 1971), Chap. 8.

39. J. Hickling and N. Wieling, "Electrochemical Investigation of the Resistance of Inconel 600, Incoloy 800, and Type 347 Stainless Steels to Pitting Corrosion in Faulted PWR Secondary Water at 150 and 250°C," Corrosion, 37, 147 (1981).

40. T. J. Murphy, "Utilization of Anodic Breakdown of Titanium Alloys as a Method of Characterization," Proc. Int. Conf. Titanium, 217, (1970).

41. H. S. Isaacs and B. Vyas, "Scanning Reference Electrode Techniques in Localized Corrosion," Electrochemical Corrosion Testing, ASTM STP 727, 3 (1981).

42. H. S. Isaacs and M. W. Kendig, "Determination of Surface Inhomogeneities Using a Scanning Probe Impedance Technique," Corrosion, 36, 269 (1980).

43. L. G. Gainer and G. R. Wallwork, "An Apparatus for the Examination of Localized Corrosion Behavior," Corrosion, 35, 61 (1979).

44. D. D. MacDonald and M. C. H. McKubre, "Electrochemical Impedance Techniques in Corrosion Science," Electrochemical Corrosion Testing, ASTM STP 727, 110 (1981).

45. B. MacDougal, D. M. Mitchell and M. J. Graham, "The Use of Electrochemical and Surface Analytical Techniques to Characterize Passive Oxide Films on Nickel," Corrosion, 38, 85 (1982).

46. "Examination and Evaluation of Pitting Corrosion," Annual Book of ASTM Standards, Part 10, Designation G46-76 (1981).

47. J. C. Griess, Jr., "Crevice Corrosion of Titanium in Aqueous Salt Solutions," Corrosion, 24, 97 (1968).

48. T. M. Ahn and P. Soo, "Container Assessment - Corrosion Study of HLW Container Materials," NUREG/CR-2317, Vol. 2, No. 1, BNL-NURG-51449, June 1982.

49. J. W. Oldfield and W. H. Sutton, "Crevice Corrosion of Stainless Steels," Brit. Corr. J., 13, 13 (1978).

50. A. J. Sedricks, Corrosion of Stainless Steels (John Wiley and Sons, 1979).

51. J. F. Bates, "Cathodic Protection to Prevent Crevice Corrosion of Stainless Steels in Halide Media," Corrosion, 29, 28 (1973).

52. M. G. Fontana and N. D. Greene, Corrosion Engineering (McGraw Hill, 1978).

53. J. W. Oldfield and W. H. Sutton, "Crevice Corrosion of Stainless Steels," Br. Corr. J., 13, 104 (1978).

54. L. L. Shreir, "Localized Corrosion," Corrosion, 1: 130 (1976) (Newnes Buttersworth, Boston).

55. K. J. Day and F. G. Dunkley, "Corrosion Testing and Determination of Corrosion Rates," Corrosion, 20:30 (1976) (Newnes Buttersworth, Boston.)

56. R. B. Diegle, "New Crevice Corrosion Test Cell," Materials Performance 21, 43 (1982).

57. E. A. Lizlovs, "Polarization Cell for Potentiostaic Crevice Corrosion Testing," J. Electrochem. Soc., 117, 1335 (1970).

58. W. D. France, Jr. and N. D. Greene, Jr., "Passivation of Crevices During Anodic Protection," Corrosion, 24, 247 (1968).

59. T. S. Lee, "A Method for Quantifying the Initiation and Propagation Stages of Crevice Corrosion," Electrochemical Corrosion Testing, ASTM STP 727, 43 (1981).

60. B. E. Wilde, "A Critical Appraisal of Some Popular Laboratory Electrochemical Tests for Predicting the Localized Corrosion Resistance of Stainless Alloys in Sea Water," Corrosion, 28, 238 (1972).

61. A. Garner, "The Use of Free-Corrosion Potential-Time Transients to Distinguish Between Pitting and Crevice Corrosion After Potentiostatic Tests," Corrosion, 34, 285 (1978).

62. H. G. Nelson, "Testing for Hydrogen Embrittlement: Primary and Secondary Influences," Hydrogen Embrittlement Testing, ASTM STP 543, 152 (1974).

63. C. R. Caskey, Jr., "The Influence of a Surface Oxide Film on Hydriding of Titanium," Hydrogen in Metals, I. M. Bernstein and A. W. Thompson, Eds. (American Soc. Metals, 465, 1974).

64. K. K. Shah and D. L. Johnson, "Effect of Surface Pre-Oxidation on Hydrogen Permeation in Alpha Titanium," Hydrogen in Metals, I. M. Bernstein and A. W. Thompson, Eds. (American Soc. Metals, 475, 1974).

65. "Hydrogen Embrittlement Testing," ASTM STP 543, (1976).

66. H. R. Gray, "Testing for Hydrogen Environment Embrittlement: Experimental Variables," Hydrogen Embrittlement Testing, ASTM STP 543, 133 (1974).

67. J. P. Fidelle, R. Broudeur, C. Pirrovani and C. Roux, "Disk Pressure Technique," ibid., page 34.

68. J. P. Fidelle, R. Bernardi, R. Broudeur, C. Roux and M. Rapin, "Disk Pressure Testing of Hydrogen Environment Embrittlement," ibid., page 221.

69. T. F. Archbold and D. H. Polonis, "Assessment of Delayed Failure Models in Titanium and Titanium Alloys," PNL-4127, Dec. 1981.

70. T. F. Archbold, R. B. Bower and D. H. Polonis, "Assessment of Predictive Models for the Failure of Titanium and Ferrous Alloys Due to Hydrogen Effects," PNL-4157, April 1982.

71. P. E. Irving and C. J. Beevers, "Some Observations on the Deformation Characteristics of Titanium Hydride," J. Mat. Sci., 7, 23 (1972).

72. R. J. Brigham, "On the Variability of Crevice Corrosion Initation in Ferric Chloride Exposure Tests," Corrosion, 37, 608 (1981).

73. N. E. Paton and J. C. Williams, "Effect of Hydrogen on Titanium and its Alloys," Hydrogen in Metals (American Soc. Metals, 409, 1974).

74. K. J. Puttlitz and A. J. Smith, "The Influence of Microstructure on the Hydrogen Embrittlement of Pure and Commerically-pure Titanium," Hydrogen Effects in Metals, I. M. Bernstein and A. W. Thompson, Eds. (AIME, 427 1981).

75. B. Siskind, "Stress Corrosion Cracking, Galvanic Corrosion and Selective Leaching Test Requirements for TiCode-12 High Level Waste Containers," BNL-NUREG-31755, August 1982.

76. T. M. Ahn, K. S. Czyscinski, E. M. Franz, C. J. Klamut, B. S. Lee, N. S. McIntyre, K. J. Swyler and R. J. Wilke, "Nuclear Waste Management Technical Support in the Development of Nuclear Waste Form Criteria for the NRC," Task 4, Test Development Review, NUREG/CR-2333, Vol. 4, BNL-NUREG-51458, Chap. 5, Feb. 1982.

77. D. A. Meyn, "Effect of Hydrogen Content on Inert Environment Sustained Load Crack Propagation Mechanisms of Ti-6Al-4V," Environmental Degradation of Engineering Materials in Hydrogen, Lab. Study of Environmental Degradation of Engineering Materials, Virginia Poly. Inst. Blacksburg, (1981).

78. R. W. Judy and R. J. Goode, "Prevention and Control of Sub-critical Crack Growth in High Strength Metals," NRL-7780, AD785233, August 1974.

79. A. H. Priest, "Experimental Methods for Fracture Toughness Measurement," J. Strain Analysis, 10, 225 (1975).

80. J. D. Landes and J. A. Begley, "The Effect of Specimen Geometry on J_{Ic}," Fracture Toughness, Proc. 1971 National Symp. Fracture Mech. Part II, ASTM STP 514, 24 (1972).

81. J. D. Landes and J. A. Begley, "Recent Developments in J_{Ic} Testing," Dev. Fracture Mech. Test Method Standardization, ASTM STP 632, 57 (1977).

82. Standard Practice for R-Curve Determination," Annual Book of ASTM Standards, Part 10, Designation E561-81, 1981.

83. R. P. Wei, S. R. Novak and D. P. Williams, "Some Important Considerations in the Development of Stress Corrosion Cracking Test Methods," Materials Research and Standards, page 25, Sept. 1972.

84. "Fatigue Precracking of K_{Ic} Fracture Toughness Specimens," Annual Book of ASTM Standards, Part 10, Designation 399-81, Annex A2, 1981.

85. W. P. Deans and C. E. Richards, "A Simple and Sensitive Method of Monitoring Crack and Load in Compact Fracture Mechanics Specimens Using Strain Gages," J. Testing and Evaluation, 7, 147 (1979). Taken from Ref. 70.

86. "Plane-Strain Fracture Toughness of Metallic Materials," Annual Book of ASTM Standards, Part 10, Designation E399-81, 1981.

87. R. R. Boyer and W. F. Spurr, "Characteristics of Sustained-Load Cracking and Hydrogen Effects in Ti-6Al-4V," Met. Trans., 9A, 23 (1978).

88. "Standard Test for J_{Ic}, A Measure of Fracture Toughness," Annual Book of ASTM Standards, Part 10, Designation E813-81, 1981.

89. G. A. Clarke, W. R. Andrews, P. C. Paris and D. W. Schmidt, "Single Specimen Tests for J_{Ic} Determination," Mechanics of Crack Growth, ASTM STP 590 (1976).

90. D. W. Dickinson and G. D. Ries, "Implant Testing of Medium to High Strength Steel - A Model for Predicting Delayed Cracking Susceptibility," Welding Research Supplement, 205s (1979).

91. C. R. Weymueller, "Applying the Right Mechanical Test Method," Welding Design and Fabrication, 56, 92 (1977).

92. R. P. Simpson and K. C. Wu, "Microstructure - Property Control with Postweld Heat Treatment," Welding Research Supp., 54, 73s (1975).

APPENDIX A

Summary of Methods of Crack Length Measurement[85]

Technique	Brief Description	Advantages	Disadvantages
Optical	relies on microscopes or telescopes, often aided by etched or scribed markings; almost all test piece geometries	inexpensive; does not require calibration; does not require specimen to behave in a linear elastic manner	only gives surface readings and usually underestimates average crack length because of crack curvature; not amenable to automation and hence time-consuming; requires surfaces to be accessible and in well-polished condition
Mechanical, COD	basis is to measure the COD, usually between points along the loading line or, in the case of bend and wedge opening loading specimens, at the front face [55-60]; displacement measured mostly by clip gages; for high temperature testing extension arms may be used to transfer the displacements to lower temperature regions for measurement; extension arms may be used via moving seals to measure displacements inside autoclaves; any test piece geometry that behaves in a linear elastic manner	cost depends on application and ranges from low cost in room temperature air to moderately expensive in high temperature aggressive environments; does not require the specimen to be visually accessible and can provide an average crack length figure; easily incorporated in automatic systems	calibration required in some cases: clip gages and to a lesser extent transducers not very robust
Mechanical, BFS	strains measured on the back face of CT or T-type WOL specimens by strain gages or possibly clip gages or transducers for large test pieces; possible use in single-edge-notched tension or three and four point bend specimens; all specimens must behave in a linear elastic manner	cost depends on application and ranges from very inexpensive in room temperature air tests to moderately expensive in high temperature aggressive environments; does not require the specimen to be visually accessible and can provide an average crack length figure; shows excellent characteristics for incorporation in automatic systems	calibration required for test pieces other than CT and T-Type WOL specimens
Electrical, strain gage filaments	electrically conducting wires are attached to the specimen so that they are broken by an advancing crack, providing stepwise changes in resistance [61-63]; can be used for all specimen geometries	low cost; easily adapted for automatic processes	only gives surface readings, not well suited for high temperatures and aggressive environments; difficult to locate gages and ensure crack always and only breaks filaments when crack tip passes through

Technique	Brief Description	Advantages	Disadvantages
Electrical, d-c potential drop (resistance)	a constant d-c current is passed through a specimen so that a change in crack length alters the potential difference of suitably placed contact points, usually in vicinity of the crack tip [55,64-67]; suitable for all test piece geometries	low cost; does not require any delicate instrumentation attached to the specimen; high stability for long term tests and some relaxation from linear elastic behavior easily accommodated; particularly well suited for automatic control and long term, high temperature testing; robust and simple; can give an average crack length value	some theoretical calibrations available but usual to carry out calibration tests; some uncertainty in stress corrosion and corrosion fatigue studies over possible interference with electrochemical conditions adjacent to crack tip; for decreasing K, constant COD tests crack faces may short electrically, thus underestimating crack length; bridging of crack surfaces by corrosion products may produce erroneous crack length readings; in some cases the grips may have to be electrically insulated from the testing machine; not well suited for very large specimens
Electrical, a-c potential drop (resistance)	similar to d-c potential drop	does not require any delicate instrumentation attached to the specimen; some relaxation from linear elastic behavior easily accommodated; well suited for automatic control and can give average crack length values; high sensitivity	moderate cost; wires have to be carefully placed and must not be moved during test; long-term stability difficult to achieve; bridging of crack surfaces by corrosion products may produce erroneous crack length readings; electrical insulation required
Electrical, eddy currents	an eddy current probe adjacent to a cracked surface produces an electrical signal, indicating the crack [68]; can be used with a servo-system or stepping motor that moves the probe so that a nil eddy current signal is maintained; used for center-cracked sheets but should be adaptable to other geometries.	easily adapted for automatic processes	may only be useful for surface measurements; expensive

Technique	Brief Description	Advantages	Disadvantages
Ultrasonic	involves transmission and reception of a high frequency sound beam intersected by a crack [69]; if probe is fixed the moving crack alters the proportion of the signal reflected by crack and the opposite boundary of the specimen; a more accurate version involves a stepping motor that moves the probe so that the strength of the signal reflected by the crack remains constant [70]; used mainly on WOL compact specimens	can be adapted for automatic processes; internal measurements of crack length; only method that can give crack profile; relaxation from linear elastic behavior easily accommodated	not well suited for small, thin specimens; expensive; cannot be used at high temperatures; not well suited to environmental testing; not a proven technique for specimens other than WOL compact specimens; difficult to achieve high resolution
Acoustic emission	involves attachment of sensing transducer to test piece that oscillates at its resonant frequency on receiving elastic stress waves from source of deformation [65]; detected emissions are then amplified, selectively filtered and conditioned, and then counted either on a periodic basis as a rate of emission or as a cumulative total; adaptable to any geometry	can be very sensitive for detecting onset of cracking	expensive, sophisticated equipment; filtering of extraneous noise from test machine and grips necessary during testing; poor correlation with crack length; signals are material-dependent